Methylmercury neurotoxicity and interactions with selenium

Sonja Gray Campbell

Thesis submitted to the

Faculty of Graduate and Postdoctoral Studies, University of Ottawa

In partial fulfilment of the requirements for a M.Sc. degree in Biology with a specialisation in Chemical and Environmental Toxicology

Department of Biology

Faculty of Science

University of Ottawa

Ottawa, Canada

Abstract

Methylmercury (MeHg) is a ubiquitous contaminant and potent neurotoxicant with no completely effective therapy, although selenium antagonises MeHg toxicity. Furthermore, nanoparticles are promising as a novel drug delivery system. We researched the potential of selenium nanoparticles (SeNPs) in antagonising MeHg neurotoxicity compared to selenomethionine (SeMet) using primary astrocyte cell cultures and examining outcomes related to oxidative stress. We found that SeNPs were more toxic than SeMet. Increasing SeNPs significantly decreased MeHg cellular uptake and MeHg significantly decreased uptake of SeNPs at the highest concentration. Finally, SeNPs alone produced significantly higher reactive oxidative species and altered the ratio of reduced-to-oxidised glutathione, but MeHg, SeMet, and co-exposures did not. There were no significant effects on glutathione peroxidase or reductase activity. This suggests that SeNPs are more toxic than MeHg in cerebellar astrocytes and that they may not be suitable as a therapy at the doses and formulation used in this research.

Résume

Le méthylmercure (MeHg) est un polluant omniprésent et une substance neurotoxique, mais il n'y a pas une thérapie complètement effective. La recherche a montré que sélénium a un effet antagonistique contre la toxicité de MeHg. De plus, les nanoparticules ont le potentiel d'améliorer les propriétés de médicaments. Nous avons recherché le potentiel de nanoparticules de sélénium (NPSe) d'antagoniser les effets neurotoxicologique du MeHg en comparant avec sélénométhionine (SeMet). Nous avons utilisé un modèle de culture cellulaire avec des astrocytes cérébelleux et étudié les effets de stress oxydant. Nous avons trouvé que les NPSe étaient plus toxiques que SeMet. Aussi, il y avait une relation inverse significative entre l'exposition des NPSe et l'absorption cellulaire du MeHg, mais pas avec SeMet, et le MeHg a diminué l'absorption cellulaire des NPSe à leur concentration maximum, mais pas SeMet. Enfin, les NPSe ont augmenté la production des dérivés réactifs de l'oxygène et diminué la proportion du glutathion réduit au glutathion oxydé. L'activité de la glutathion peroxydase et la glutathion réductase n'a pas changé entre les doses différentes. Ces résultats suggèrent que les NPSe sont plus toxiques que le MeHg pour les astrocytes cérébelleux et qu'ils ne sont pas appropriés comme une thérapie aux doses et formulations utilisant dans ces expériences.

List of Tables

List of Figures

Glossary

Astrocytes: A type of glial cell, they are support cells in the brain that help maintain proper neuronal function and homeostasis.

Antagonist: A chemical that interferes with the biochemical mechanism of another, leading to a reduction in its effects.

Antioxidant: A chemical that neutralises free radicals and other cellular oxidising agents, reducing cellular oxidation.

Blood-Brain Barrier: a selective membrane that allows passage of only small lipophilic compounds that can diffuse across membranes and ions and metabolic products via specific active transporter proteins.

Cerebellum: A part of the central nervous system, it is classified as part of the metencephalon and is responsible for motor control.

Chronic exposure: Exposure to a compound over a long time; doses may be high or low.

Dose: The amount of a chemical that is taken up and absorbed by an organism.

Exposure: The concentration of a chemical that an organism is exposed in the ambient environment, including air, water, or soil.

Mechanism of action: The biochemical and molecular interactions of a xenobiotic with an organism by which it elicits its effects.

Nanoparticle: Aggregates of a compound between 1–1000 nm in at least one dimension, although more stringent definitions require 1–100 nm in at least one dimension.

Neurotoxicant: A xenobiotic that has an adverse effect on the nervous system.

Oxidative stress: An imbalance of the cellular redox system that results in high levels of reactive oxygen species that cause cell damage and can lead to cell death.

Primary cell culture: Cells cultured in an artificial support medium that have originated directly from live tissue.

Reactive oxidative species: highly reactive oxidative compounds produced as a bi-product of mitochondrial respiration.

Sublethal: Doses lower than the threshold to cause death in a significant proportion of the population exposed.

Toxicant: A chemical with toxic properties that originates from an anthropogenic source.

Toxicodynamics: The properties of the interactions of a toxic xenobiotic with an organism, such as its mechanism of action that elicits toxicity.

Toxicokinetics: The properties of the interactions of an organism with a toxic xenobiotic, including its absorption, distribution, metabolism, and excretion.

Xenobiotic: A compound found in a system, including the environment or within an organism, which has not been produced by that system.

Abbreviations

ASM	Astrocyte specific media
BSA	Bovine serum albumin
DMSO	Dimethyl sulfoxide
DTT	dithiothreitine
EDTA	tetrasodium ethylenediaminetetraacedic acid
ETC	Electron transport chain
FBS	Fetal bovine serum
GABA	Gamma aminobutyric acid
GPx	Glutathione peroxidase
GR	Glutathione reductase
GSH	Glutathione
GSSG	Glutathione disulphide
HBSS	Hank's balanced salt solution
HPLC	High performance liquid chromatography
ICP-MS	Inductively coupled plasma mass spectrometry
LDH	Lactose dehydrogenase
LOEL	Lowest observed effects level
MDMA	3,4-methylenedioxy-methamphetamine
MeHg	Methylmercury
MeHgCl	Methylmercury chloride
MPTP	1-methyl-4-phenyl-1,2,3,6-tetrahydropyridine
mtCK	mitochondrial creatine kinase
MTT	3-(4,5-dimethylthiazol-2-yl)-2,5-diphenyltetrazolium bromide (tetrazolium dye)
NAC	N-acetyl cysteine
NADPH	Nicotinamide adenine dinucleotide phosphate
NPSH	Non-protein sylfhydryl
PBS	Phosphate buffered saline
PSP	Polysaccharide-protein complex
Se	Selenium
SeMet	Selenomethionine
SeNP	Selenium nanoparticle
TBARS	thiobarbituric acid reactive substances
TrxR	thioredoxin reductase
UNEP	United Nations Environmental Programme
US EPA	United States Environmental Protection Agency

Acknowledgements

This work is the product of collaboration of many people. The objectives of this project were developed with the help of my supervisor, Dr. Laurie Hing Man Chan. Furthermore, he provided guidance into the methodology, including: MeHg dosing concentrations and the dosing regime of the co-exposures; the rationale to include the cell uptake experiments; advice on data analysis and presentation; and critiques on the final thesis. My graduate committee members, Dr. Michael Jonz, Dr. Bill Willmore, and Dr. Alexandre Poulain provided valuable guidance throughout the course of my thesis. Dr. Ryan Mailloux provided the suggestion to include the 2GSH/GSSG experiment in the experiment in place of a less sensitive method. Also, he measured the 2GSH/GSSG samples and completed the data processing. Finally, Dr. Ryan Mailloux provided invaluable advice on the enzyme assays that allowed us to optimise the experiments effectively. Dr. Emmanuel Yumvehoze provided advice on the cell uptake methodology, in particular helping to optimise the selenium uptake experiment, which initially had issues with instrument sensitivity. As well, he conducted the measurements and initial data processing of the results for the selenium uptake samples. Finally, Yueting Shao provided training on primary astrocyte culturing techniques; in addition, she helped to trouble shoot cell culturing problems and provided cell culturing-related advice for these experiments.

This project was funded by NSERC.

Table of Contents

1. Introduction

While all forms of mercury are toxic, methylmercury (MeHg) is of most concern for public health due to its toxicity and ubiquity in the environment (Fitzgerald *et al*., 2007). As well, it is more bioavailable and has a longer half-life in the body than other forms of mercury (Clarkson *et al*., 2003). While some therapies, such as chelators, have limited success for inorganic mercury poisoning (Carvalho *et al.,* 2007; Mitka, 2008), there is no completely effective or recommended therapy for MeHg poisoning. Selenium is an essential metalloid micronutrient that has been shown experimentally to antagonise MeHg toxicity due to its importance in antioxidation pathways as well as a strong binding affinity with MeHg. Because of this, selenium is promising as a therapy for MeHg neurotoxicity. In particular, selenium nanoparticles (SeNPs) may have an application as a therapy against MeHg neurotoxicity, although no research has examined this.

Research on methylmercury neurotoxicity and mercury-selenium interactions has been ongoing for decades and an exhaustive review would be impractically long. However, this literature review covers sufficient research to understand the current state of knowledge on MeHg and selenium research. The following section describes the current knowledge of sources, exposure, and neurotoxicity of MeHg in humans, the biological role of selenium, its interactions with MeHg and significance with MeHg-induced neurotoxicity, and potential as a therapeutic agent, with a focus on SeNPs. This is followed by the rationale, objectives, and hypotheses for my research, examining the effects SeNPs on MeHg neurotoxicity.

1.1. Literature review

1.1.1. Environmental sources of MeHg

Methylmercury originates from inorganic mercury. Mercury occurs naturally in its elemental form (Hg^0) in ores, coal, and oil (UNEP, 2013a). Weathering and leaching of deposits, volcanic eruptions, and geothermal activity are natural sources of Hg, with atmospheric emissions of Hg^0 considered the most significant type produced. Due to its high volatility, Hg^0 travels long distances on atmospheric wind currents and is oxidised abiotically to divalent mercury (Hg^{2+}), which deposits onto the Earth. Globally, Hg^{2+} deposition occurs disproportionately more in the Arctic due to wind patterns (Lindberg *et al*., 2002).

Oceans serve as large reservoirs for mercury. It is rapidly absorbed into the upper layer of the water column and slowly accumulates in deep waters, with the major accumulation zone located approximately 100–500 m below sea level (Fitzgerald *et al*., 2007; UNEP, 2013a). Near-shore marine waters and inland waters are the primary sources of MeHg via methylation of divalent mercury. While this occurs biotically and abiotically (Fitzgerald *et al*., 2007; Selin, 2009), it is primarily mediated by sulfate-reducing and iron-reducing bacteria in anoxic aquatic sediment (Compeau & Bartha, 1985).

Historically, mercury was used in numerous applications and emitted in waste effluent without regulations (Fitzgerald *et al*., 2007; UNEP, 2013a). With increasing appreciation of its toxicity, it has been phased out of use. It is still used in limited industries

and anthropogenic mercury sources include fossil fuel production and combustion, as well as mining and artisanal gold production. Anthropogenic emissions have increased the global biogeochemical mercury load. Over the past 100 years, mercury levels in the upper and deep ocean waters have increased by 100 and 10–25%, respectively (UNEP, 2013a).

On most continents, anthropogenic mercury emissions are declining due to increasingly stringent regulations; however, they are increasing in East and Southeast Asia, which account for nearly 40% of global anthropogenic atmospheric emissions (UNEP, 2013a). Increased emissions in Asia have consequences in other regions. Due to its atmospheric persistence and transportation, mercury is a long-range trans-boundary air pollutant, which impedes the ability to target specific mercury sources. Therefore, a global effort to reduce mercury emissions is necessary to yield a global decrease in the mercury load. In January 2013, the United Nations Environmental Programme Minamata Convention on Mercury agreed on negotiations of a legally binding treaty to stop global anthropogenic mercury emissions. The treaty will be enacted around 2016–2018, with some components of the phase-out taking longer (UNEP, 2013b). Furthermore, due to the persistence and environmental load of mercury, the lag time between reducing global anthropogenic emissions and seeing the effects in the environment could take years to decades (UNEP, 2013a). Therefore, mercury will remain a health concern for decades.

1.1.2. Human exposure and epidemiology

Fish and seafood are the primary sources of human MeHg exposure. Once MeHg is produced, it adsorbs to organic matter, including suspended organic particulates and plant matter and is deposited primarily in edible tissue, including muscle and soft organs. It readily enters the aquatic food web and bioaccumulates and magnifies up trophic levels (Selin, 2009). As well, it has a high bioavailability; greater than 90% of MeHg is absorbed from the gastro-intestinal tract into the bloodstream. In marine food webs, the highest concentrations of mercury are found in piscivorous predators near the top of the food chain, including swordfish and tuna, as well as predatory marine mammals (Clarkson *et al*., 2003).

The US Environmental Protection Agency (US EPA) has set a reference dose of 0.0001 mg MeHg/Kg/day in adults and 0.00001 mg/Kg/day during developmental stages (US EPA, 2001) and species-specific fish consumption advisories are available to help consumers minimise their exposure to mercury while maintaining the health benefits from fish consumption (US FDA, 2013a). While fish consumption provides many health benefits, some edible piscivorous fish samples have been found containing MeHg concentrations that exceed safe exposure levels (Clarkson *et al*., 2003; Hachiya, 2012). This places populations that rely on fish and seafood as a dietary staple, at risk of MeHg toxicity.

Methylmercury is toxic to numerous organ systems; however, the brain is the primary target of toxicity (Clarkson *et al*., 2003). The neurological dysfunction caused by severe MeHg poisoning is called Minamata disease, named after a widespread poisoning caused by environmental pollution in Minamata Bay, Japan. For decades, a chemical manufacturer,

Chisso Inc., dumped its liquid effluent into Minamata Bay, which was found to contain high MeHg levels. Marine fish and shellfish, staple foods of the local population, became severely contaminated, poisoning many who consumed it. Minamata disease was officially documented in 1956 (McAlpine & Araki, 1958), although reports of symptoms began in the early-1950s (Harada, 1995). Only 34 adults were initially diagnosed with Minamata disease. However, from the late 1950–60s, many infants were born with brain and neurological defects, while mothers were often asymptomatic, or showed only mild symptoms of Minamata disease (Harada, 1978; Harada, 1995). Although acute and sub-acute cases of Minamata disease began to decrease in the 1960s, chronic toxicity remains an issue, manifesting in several forms. Many patients who were initially diagnosed with slight symptoms worsened. In other cases, other diseases exacerbated symptoms. Continuing research on the aging population of Minamata, Japan has found the even those who did not exhibit symptoms during the crisis appear to be at greater risk for developing neurodegenerative diseases later in life (Harada, 1995).

Much can be learned about MeHg neurotoxicity from the Minamata Bay poisoning. Toxicity can occur from acute high exposure and chronic high and low exposure. High exposures can take months and chronic low exposures decades for symptoms to present, making early diagnosis difficult. Symptoms of acute and chronic high exposure include paresthesia of the extremities and circumoral area, visual constriction, and ataxia (Clarkson *et al*., 2003). While chronic low MeHg exposure can appear asymptomatic for decades, it has been linked with increased risk of developing neurodegenerative diseases (Migliore & Coppedè, 2009). Moreover, MeHg is more toxic from *in utero* exposure than in adults.

Although poisonings are rare, many other epidemiological studies have examined low-exposure MeHg toxicity in at-risk populations that rely on seafood as a dietary staple, including populations in Northern Canada, Greenland, Seychelles, Faroe Islands, New Zealand, and Japan (Castoldi *et al*., 2008). It has been identified as a potential risk factor for neurological disorders, including neurodevelopmental delays (Grandjean *et al*., 1997; Sorensen *et al.*, 1999; Steuerwald *et al*., 2000) and neurodegenerative diseases (Migliore & Coppedè, 2009). However, some evidence contradicts these findings, complicating the epidemiological evidence. For example, Petersen *et al.* (2008a) found no correlation between MeHg exposure and Parkinson's disease. Conversely, the incidence of Parkinson's disease in the Faroe Islands is two times greater than average and a study found that co-exposure to MeHg and polychlorinated biphenyls was correlated positively with Parkinson's disease (Petersen *et al*., 2008b). Moreover, cohort studies have linked foetal exposure to developmental delays. Maternal MeHg cord blood and hair levels and child development based on neuropsychological and intelligence domain parameters were examined in the Faroe Islands. Methylmercury levels were correlated with a delay in specific developmental parameters, including memory, at age 7 (Myers *et al*., 2000). In the Seychelles Development Study some deficits in fine motor function were observed at age 9 (Davidson *et al*., 2006).

Although there are some conflicting reports, epidemiological evidence supports that MeHg has neurotoxic outcomes, in particular in from exposure *in utero*. Despite some conflicting evidence, as well as the difficulty of dealing with confounding factors, the general consensus of epidemiological evidence on MeHg exposure is that normal chronic environmental exposure on the high end of the spectrum is associated with developmental delays in children and neurodegenerative diseases in elderly adults.

1.1.3. Mechanisms of MeHg neurotoxicity

The brain is the primary target of MeHg and accounts for many of the clinical symptoms and complications described above. High exposures can result in apoptotic and necrotic cell death, ultimately leading to brain lesions (Wakabayashi *et al*., 1995); however, even sublethal exposures can have detrimental effects. In part, its targeted effects on the brain can be explained by distribution. By weight, a higher proportion of MeHg accumulates in the brain than expected (Yamamoto *et al*., 1986) and can distribute differently among brain regions (Evens *et al*., 1977). Initially, it is found more as organic mercury, although demethylation has been demonstrated (Shapiro & Chan, 2008). Unlike other forms of mercury, MeHg can cross the blood-brain barrier (Simmons-Willis *et al*., 2002). Once in the brain, MeHg distribution may influence its toxicity. Accumulation has been shown to be region-specific, with hotspots in the cerebral cortex and cerebellum (Castoldi *et al*., 2000), which mirrors where toxicity occurs.

Methylmercury has been shown to have widespread sublethal effects in the brain. Experimental evidence has shown effects on multiple neurotransmitter systems, including the glutamatergic, dopamine, cholic, and gamma-aminobutyric acid (GABA) systems (Brookes & Kristt, 1989; Coccini *et al*., 2000; Götz *et al*, 2002; Basu *et al*., 2007). Excitatory neurons that use glutamate, such as cerebellar granular neurons and optic fibre neurons are especially susceptible, possibly due to MeHg-induced excitotoxicity (Juárez *et al*., 2002). It has also been shown to have effects on multiple sub-cellular systems, such as calcium deregulation, mitochondrial dysfunction, and disruption of tubulin and microtubules (Berg *et al*., 2010). While region- and target- specific mechanisms may differ and the full mechanism of its

toxicity has not been elucidated, there are two mechanisms that have widespread influence on its toxicity, binding with thiols and induction of oxidative stress. These mechanisms of its neurotoxicity are described below, with particular focus on sublethal outcomes.

Thiol Binding

Thiols (-SH) are a common biological reactive group that are prevalent in proteins. Mercury has a strong binding affinity with thiols, greater than for most other biological ligands (Hughes, 1957), with association constants in the range of 10^{15}–10^{17} depending on the specific compounds (Simpson, 1961). Their association has been described as strong but labile, as mercury readily exchanges bonds between thiols (Rabenstein & Reid, 1983).

These characteristics are important in the mechanisms that drive the toxicokinetics and -dynamics of MeHg. Once MeHg enters the bloodstream, it binds rapidly to serum proteins via thiols (Fang & Fallin, 1976), facilitating its distribution through the body and cellular uptake. For example, cellular absorption and mobility in the bloodstream has been correlated with glutathione (GSH) and metallothionein levels, thiol-containing molecules that have roles in detoxification (Foulkes, 1993). As well, binding with cysteine, a thiol-containing amino acid, allows MeHg to cross the blood-brain barrier. The MeHg-cysteine complex mimics the shape of the amino acid methionine (Aschner & Aschner, 1990; Kerper *et al*., 1992) and allows for active transportation across the blood-brain barrier via L-system amino acid carriers that normally transport methionine (Simmons-Willis *et al.*, 2002). By a similar mechanism, MeHg-cysteine is important for cellular uptake via L-system amino acid transporters (Aschner *et al*., 1990).

Thiols could also act as molecular targets for MeHg toxicity, driving its toxicodynamics. Since thiols are prevalent in the body in proteins, this partly explains the widespread toxic effects of MeHg, as MeHg can bind and possibly alter or inhibit the function of proteins and peptides (Farina *et al*., 2011a). Supporting this, some studies have found altered cellular free thiol status in neural cells exposed to MeHg (Franco *et al*., 2006; Berg *et al*., 2010; Sumathi *et al*., 2012). For example, GSH is the major antioxidant in the body and is also important in detoxification and elimination pathways. It is a tripeptide that contains a thiol-containing cysteine. In the brain, MeHg has been shown to inhibit cysteine in astrocytes and neurons, thereby limiting cellular GSH formation and the antioxidation capacity of neural cells (Shanker & Aschner, 2001; Franco *et al*., 2006).

Oxidative Stress

Stoichiometric interactions with thiols cannot fully explain the toxicity of MeHg, since sublethal toxicity of MeHg has been observed in the sub- and low-micromolar range, while cellular thiols are present in the millimolar range (Farina *et al*., 2011a). Another explanation for the widespread effects of MeHg that accounts for this difference is its effects on cellular redox balance. Methylmercury neurotoxicity induces cellular oxidative stress, which can have acute and chronic effects. Several researchers have even suggested that MeHg-induced oxidative stress is the primary mechanism for toxicity (Farina *et al*., 2011b), and could possibly explain the associations between chronic MeHg exposure and neurodegenerative diseases (Migliore & Coppede, 2009). The induction of oxidative stress in MeHg neurotoxicity is caused by both an increase in ROS production and a depletion of

cellular antioxidants. An overview of possible interactions of MeHg within cells related to cellular oxidative stress is shown in Figure 1.1.

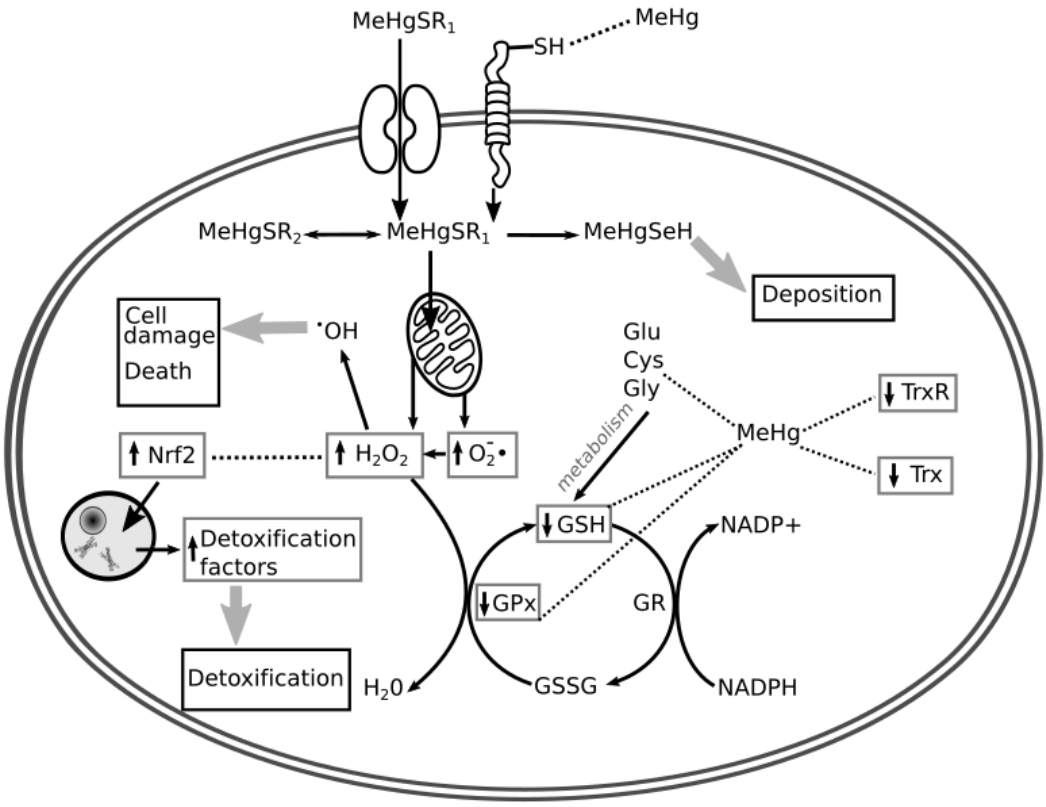

Figure 1.1: Effects and outcomes of MeHg on cellular redox systems. (1) MeHg can enter cells through transmembrane transporters bound to proteins by their cysteine residue. It is also thought to cross by binding with cysteine residues on transmembrane proteins, binding with multiple residues along the protein and ultimately entering the cell. Within cells, MeHg can jump from thiol to thiol and also bind with selenol groups. (2) MeHg has been shown to cause mitochondrial dysfunction, in particular on complex II and III of the electron transport chain, increasing the output of superoxide anions peroxides and peroxides, which lead to the formation of hydroxyl radicals, causing widespread cellular damage and potentially triggering cell death in sufficient quantities. There is evidence that peroxide production also stimulates increased levels of Nrf2, which can increase gene transcription of detoxification proteins. (3) MeHg also decreases antioxidant capabilities of cells, with influences on the glutathione redox cycle, as well as the antioxidant Trx and related enzymes. Image adapted from Farina *et al*., 2011b.

Reactive oxidative species (ROS) are a direct product of cellular respiration. They can cause oxidative damage resulting in DNA damage and mutations, protein damage, and lipid peroxidation (Yin *et al.*, 2006) and sufficiently high ROS levels can trigger apoptosis or necrosis. In the brain, MeHg has been shown to increase ROS production and induce oxidative stress by several means. First, MeHg has been shown to cause mitochondria dysfunction, which increases ROS production (Mori *et al*., 2007, Dreiem *et al*., 2005). For example, cerebral astrocyte cultures exposed to 10 μM MeHg and examined with fluorescence probes over time showed that ROS increased initially near the mitochondria, after which whole-cell ROS levels increased (Shanker *et al*., 2004).

Within mitochondria, there is evidence that MeHg targets the electron transport chain, which is integral to energy production as well as ROS production. One study showed that mitochondria exposed to MeHg had lower oxygen consumption but higher ROS production, leading to the suggestion that complexes II and III were particular susceptible to its effects (Mori *et al*., 2007). This was confirmed by Glaser *et al*., (2010), who found effects on complexes II and III, as well as I and IV. Mori *et al*., (2010) suggested that this could be due to functional modification of these proteins by MeHg, which could potentially bind to thiols present in the proteins and alter their function. In addition to thiols, the electron transport chain complexes contain iron-sulphur clusters, which are important to their function. Several inorganic studies have found that divalent mercury can compete with the iron for binding sulphur in these groups (Jeong *et al*., 2007; Skyllberg & Drott, 2010). Using *Escherichia coli*, Xu and Imlay (2012) found that soft metals, including divalent mercury, targeted iron-sulphur clusters, inhibiting enzyme function. Finally, one study suggested that

MeHg could react with iron sulphur clusters at biological pHs (Arakawa *et al*., 1980). However, more research is required to confirm the interactions between MeHg and electron transport chain proteins.

As well, mitochondria permeability transition pores have been implicated in its effects on mitochondria. A study using neonatal mouse cerebellar granule neurons showed that exposure to 0.5 μM MeHg resulted in an influx of calcium ions, leading to a depolarisation of the mitochondria membrane. The authors suggested that the change to the mitochondria transition pores could be through direct binding of MeHg to thiols on the pore (Limke and Atchison, 2002).

In discussing MeHg neurotoxicity, it is important to differentiate among brain regions and cell types. Differential effects on oxidative stress could also explain why MeHg has different effects among regions of higher accumulation, in particular between the cerebellum and the cortex. In a study that examined markers of oxidative stress between the cerebral cortex and cerebellum of rats that had been fed 10 mg/kg MeHg for 5 days, the cerebellum had higher ROS production and oxygen consumption and lower mitochondrial GSH stores than cerebral tissue. Furthermore, they found that only cerebellar mitochondria exhibited lower oxygen consumption (Mori *et al*., 2007). Mitochondria function has also been shown to differ in different regions of the brain. Since MeHg targets mitochondria, this could help explain different toxicities by brain region (Friberg *et al*., 1999).

Another factor that could cause effects to differ by brain region is cell composition within different brain regions, as it has been shown that there are differences in toxicity

among neural cell types. In, particular, brain regions with more excitatory glutamatergic neurons, such as the cerebral cortex, frontal cortex, and the cerebellum, have been shown to be highly sensitive to MeHg (Bal-Price & Brown, 2001; Juarez *et al*., 2005; Xu, *et al*., 2012). This is likely due to induction of excitotoxicity, where excess release by pre-synaptic neurons and inhibited removal by astrocytes of the excitatory neurotransmitter glutamate into neuron synapses leads to excess downstream calcium signalling and ROS production, which can trigger oxidative stress and neuronal death (Choi, 1985; Bal-Price & Brown, 2001; Juarez, *et al*., 2002; Mutkus *et al*., 2005).

Besides increasing ROS production, MeHg has also been shown to deplete cellular antioxidants and lower activity of related enzymes. Glutathione, the predominant antioxidant in the body, reduces peroxides to water through the GSH redox cycle, relying on two enzymes, glutathione peroxidase (GPx) and glutathione reductase (GR). Methylmercury has been shown to deplete GSH levels independent of ROS production, which inhibits cellular antioxidation capacity and further increases ROS in both neurons and astrocytes (Kaur *et al*., 2006; Lu *et al*., 2011; Shanker & Aschner, 2001). Methylmercury has also been shown to affect the enzymes that drive the GSH redox cycle. While MeHg decreases activity of GPx, most studies have found no effects on GR (Franco *et al*, 2009; Branco *et al*., 2012; Sakamoto *et al*., 2013). An *in vivo* study on mice found that mice supplemented with 40 mg/L MeHg for 21 days had significantly lower GPx activity in their cortex and cerebellum and activity in the cerebellum was lower than in the cortex (Zemolin *et al*., 2012). Western blot analysis indicated that GPx isozymes 1 and 4 were lower in the cerebellum compared to the control, but only GPx4 was reduced in the cortex, possibly explaining the difference between the two brain regions. The same study showed that GR, glutathione s-transferase, catalase, and

superoxide dismutase activity were higher in the cerebellum in the MeHg-exposed group, but only catalase was significantly higher in the cortex (Zemolin *et al*., 2012).

Methylmercury has been shown to inhibit other antioxidant systems. For example, thioredoxin is involved in redox signalling and has been implicated in ROS production (Nordberg *et al*., 2001). Methylmercury has been shown to decrease thioredoxin and thioredoxin reductase, a key enzyme in this process. In one study, thioredoxin reductase activity decreased in both the cerebellum and the cortex after MeHg exposure (Zemolin *et al*., 2012). In addition, chronic low MeHg exposure in zebra seabreams led to a decrease in both thioredoxin and thioredoxin reductase in the brain (Branco *et al*., 2011).

Methylmercury-induced oxidative stress is central to MeHg neurotoxicity. Oxidative stress has widespread sublethal toxic effects and helps to explain some of the clinical signs of MeHg toxicity. Although the full mechanism of MeHg neurotoxicity has not been determined, oxidative stress has been suggested as the dominant mechanism that drives its neurotoxicity; however, further research is necessary to clarify this.

1.1.4. The biological role of selenium

Selenium is an essential metalloid micronutrient. In mammals, it is incorporated into two amino acids: L-selenocysteine and seleno-L-methionine (SeMet). These are analogous to cysteine and methionine, respectively, with selenium replacing sulphur. The selenium in selenocysteine occurs as a selenol (-SeH) substituent group, analogous to a thiol group.

When selenocysteine is incorporated into proteins, it is used in the active site and alters protein function. Since enzymes containing selenocysteine require it for proper functioning, they are called selenoproteins or selenoenzymes. While both selenol and thiol groups are nucleophilic, selenium is more nucleophilic and reactive than sulfur (Bachrach *et al*. 2004; Steinmann *et al*., 2010). Conversely, SeMet can be interchanged with methionine in proteins without altering protein functioning and is considered a form of selenium storage (Burk *et al*., 2001).

There are a number of mammalian enzymes that are selenoenzymes. Enzymes with multiple isozymes include: glutathione peroxidases, thioredoxin reductase (TrxR), and thyroid hormone deiodinases. Other selenoenzymes include: selenoproteins H, I, K, M, N, O, P, R, S, T, U, V, and W; methionine-R-sulfoxide reductase 1; 15 kDa selenoprotein; and selenophosphate synthetase 2 (Behne & Kyriakopoulos, 2001; Burk *et al.*, 2001; Arner, 2009). Many selenoenzymes are involved in pathways related to antioxidation, including GPx, TrxR, and selenoprotein P (Cohen & Hochstein, 1963; Steinbrenner *et al*., 2006; Arnér, 2009). Glutathione peroxidases are one of the most prevalent selenoenzymes. Of the eight isozymes, five contain selenocysteine at the active site in most mammals, GPx 1, 2, 3, 4 and 6. Interestingly, in many rodents, GPx6 does not occur as a selenoenzyme. All GPx isozymes are important in antioxidation. Of these, GPx 1 and 4 are found in all tissues throughout the body, including the brain, and reduce hydroperoxides. Found in the cytosol of cells, GPx1 is the most prevalent of the glutathione peroxidases and is responsible for oxidising GSH in the glutathione redox cycle (Brown & Arthur, 2001). The other GPx selenoenzymes are tissue-specific and not found in the brain: GPx2 is found in gastrointestinal epithelial tissue, GPx3

is formed in the kidney and secreted into the bloodstream, and GPx6 is found in olfactory tissue.

Experimental evidence indicates that selenium is important in brain functioning. In general, *in vivo* studies have shown that a diet sufficiently low in selenium to deplete selenium in most body tissues does not significantly decrease selenium levels in the brain (Savaskan *et al*., 2003). In addition, after supplementation of selenium in deficient animals, a large proportion of the selenium is distributed to the brain (Trapp & Millem, 1975). This suggests that brain selenium levels are well regulated. As well, inducing a general selenium deficiency or deficiency of specific selenoproteins in the brain has been linked to neurological injury, including seizures and susceptibility to neurotoxic xenobiotics. Several studies have shown that selenium deficiency in the brain can exacerbate neurological damage by neurotoxicants, including MeHg (Savaskan *et al*., 2003), methamphetamine (Imam *et al*., 1999), MPTP (Vizuete *et al*., 1994), and MDMA (Sanchez *et al*., 2003), suggesting that selenium is important in protecting the brain from damage. In addition, it has been hypothesised that selenium deficiency in the brain could increase susceptibility to neurological disorders and diseases (Chen & Berry, 2004; Schweizer *et al*., 2004; Valentine *et al*., 2008), including Parkinson's disease, Alzheimer's disease, and seizures. In these cases, it has been shown that damage is ROS-mediated, since selenium is important in antioxidation and deficiency can decrease ability to scavenge ROS and free radicals. Finally, Zhang and colleagues (2010) have suggested that selenium could be important in aging and brain health, based on the role of selenium in antioxidation and oxidative-stress related aging. In addition, they hypothesized that, similar to other antioxidants, selenium could protect against telomere-related aging.

Research on the physiological role of selenium has shown that it is important in antioxidation, in particular in brain health. However, many aspects of its role in human health remain unknown and research is ongoing to further clarify its significance in health.

1.1.5. Mercury-selenium interactions

Research on the interactions between MeHg and selenium dates back to 1972 (Ganther *et al*., 1972), with a report that dietary selenium attenuated MeHg toxicity in Japanese quail, preventing death at MeHg concentrations that induced death in the selenium-deficient group. Similar results have been observed in many studies since, with increasing focus on sublethal outcomes and environmentally relevant exposure forms and levels of MeHg and selenium. Table 1.1 shows a summary of selected results from studies that examined mercury-selenium co-exposures using *in vivo* models. Moreover, many *in vitro* experiments have been conducted to determine the underlying mechanisms of their interactions. Despite over 40 years of research, the full mechanism and significance of the interactions of selenium and mercury in MeHg toxicity have not been determined. Further complicating this, there is no epidemiological evidence that can confirm their interactions and relation to health at a population level (Choi *et al.*, 2008). However, there are several hypotheses to explain their interactions and this section describes the experimental evidence and hypotheses of selenium-mercury interactions.

Table 1.1: Review of experimental results of MeHg co-exposure with selenium examining parameters of MeHg neurotoxicity. A selection of results from *in vivo* experiments using selenium and methylmercury co-exposures to explore the interactions between selenium and methylmercury in MeHg neurotoxicity. *Se* = selenium, *Hg* = mercury, *MeHg* = methylmercury, *GPx* = glutathione peroxidase, *NAC* = N-acetyl cysteine, *DTT* = dithiothreitine, *SeMet* = selenomethionine, *GSH* = glutathione, *TrxR* = thioredoxin reductase, *GR* = glutathione reductase, *ETC* = electron transport chain, mtCK = mitochondrial creatine kinase, *TBARS* = thiobarbituric acid reactive substances *NPSH* = non-protein sulfhydryl, *AChE* = acetylcholinesterase, *ATP* = adenosine triphosphate.

Se Form & Dose	Hg Form & Dose	Exposure	Model	Outcomes	Ref.
Selenium 0.5 mg/2mL/kg in water	MeHgCl in olive oil 1.5 mg/5mL/kg	21 d MeHg + 5 d Se, Se+NAC, or Se+DTT	3 month old male rats	*MeHg increased lipid peroxidation, decreased GPx, and histological changes in liver, kidney, and brain. *Se showed amelioration, but Se+NAC and Se+DTT showed better results than Se alone.	Joshi *et al.* 2014
SeMet 0.7 or 10 mg/kg in food	MeHgCl 0.05 or 12 mg/kg in food	Post-fertilised females, 78–97 d	Zebra-fish embryos	*Increasing MeHg downregulated ¼ of all selenoprotein genes, in particular those related to antioxidation. Elevated Se prevented this.	Penglase *et al.*, 2014
SeMet control or 2 g/kg/d in water	MeHgCl 0 or 8 mg/kg/d in water/milk	Se followed by MeHg with 30 min delay for 10 d	Postnatal day 14 mouse pups	*Co-exposed pups heavier than MeHg-alone. *Cerebral total and inorganic Hg levels higher after co-exposure than just MeHg. *Cerebral Se highest in co-exposure, followed by se alone. No differences in MeHg from control. *Cerebral GSH levels did not differ among all groups, but GPx activity decrease with MeHg.	Saka-moto *et al.*, 2013
Se 10 *μ*g/L in water	MeHgCl 2 *μ*g/L in water	28 d co-exposure followed by 14 d with Se or water	Juvenile zebra sea-bream	*Lower brain MeHg in co-exposure group than MeHg-only group. *MeHg decreased Se significantly while co-exposure was same as control. *MeHg and co-exposure decreased TrxR activity.	Branco *et al.*, 2012

Se Form & Dose	Hg Form & Dose	Exposure	Model	Outcomes	Ref.
				*No effects on GR, but MeHg and co-exposure decreased GPx activity with MeHg having the greater effect	
SeMet 1.3 mg/kg	MeHg-cysteine 2.6 mg/kg	Maternal diet throughout pregnancy	15 day old mice	*8 genes responded to Se, 5 to MeHg, 63 to co-exposure. *MeHg influenced functional classes related to stress, immune, cell differentiation, cytoskeleton, and morphogenesis. *Functional classes of affected genes in co-exposure included immune system and cell adhesion.	Java-shanker *et al.*, 2011
Sodium selenite 5 *μ*mol/kg/d *sc* injection	MeHgCl 50 mg/L in water	21 d	Adult male rates	*MeHg inhibited ETC complexes I, II, II-III, and IV and mtCK activity. Se partly prevented this. *MeHg increased lipid perodidation & GR activity and decreased GPx activity in cortex and co-exposure did not prevent this. *Percent of cells with metal deposition was significantly higher in MeHg groups and this was prevented by co-exposure	Glaser *et al.*, 2010
Diphenyl di-selenide 0.4 and 1 mg/kg/d *sc*	MeHgCl 2 mg/kg/d oral	35 d	Adult mice	*MeHg increased TBARS and decreased NPSH in cerebellum and cerebrum, which Se protected in cerebrum. *Se decreased cerebellar and cerebral Hg deposition.	De Freitas *et al.*, 2009
Sodium selenite 0.06 or 0.6 mg/kg in food	MeHgCl 0.5 or 5 mg/L in water	20 d Se, then 21 d MeHg in pregnant rats	Young rats exposed *in utero*	*High MeHg + Se increased Se brain levels at 6 months. *Brain Se decreased with increasing MeHg alone in neonates	Newland *et al.*, 2006
Se 0.02, 0.05 or 0.4 mg/kg in food	MeHgCl 5 or 9 mg/kg	Se diet in pregnancy MeHg on gestation days 12-14	Neonatal mice	*Marker scores for motor ability were greater in pups exposed to high maternal Se and Hg than with low or deficient Se. *Se did not alter brain Hg levels. *MeHg decrease Se brain levels and GPx activity.	Wata-nabe *et al.*, 1999

Se Form & Dose	Hg Form & Dose	Exposure	Model	Outcomes	Ref.
SeMet 10 mg/kg in food	MeHgCl 10 mg/kg in food	10 weeks	18-month male mallard ducks	*Brain G-6-PDH levels were significantly lower in MeHg-only than co-exposed groups and control. *Mehg, Se, and co-exposure groups had increased TBARS. *Se higher in co-exposure than Se-only groups. *Hg lower in co-exposure than MeHg-only groups.	Hoffman & Heinz, 1998
Sodium selenite 1.3 mg/kg in food	MeHgCl 2 and 6 mg/kg	Se 8 weeks before mating in females until lactation + MeHg on gestation days 6-9	Rat offspring	*Brain Hg lower in the Se-exposed pups than the control, but no differences between MeHg and co-exposure. *In highest MeHg group, co-exposure with Se increased locomotion mean and rearing mean in offspring compared to MeHg only, which was lower than the control.	Fredrik-sson *et al.*, 1993
Sodium selenite 20 μmoles/kg *sc* injection	MeHgCl 20 μmoles/kg intra-peritonial injection	One MeHg dose with one Se dose 1 hr later	Male rats	*Se formed complex with MeHg. *Brain Hg levels higher with co-exposure than MeHg alone.	Masu-kawa *et al.*, 1982
Sodium selenite 0, 0.25, & 10 μmoles/kg injection	MeHgCl 0, 1, 10 & 38 μmoles/kg injection	One dose of Se. One dose of MeHg 72 hr before sacrifice	1- and 5-week old rats	*MeHg exposure shifted Se from cytosol to mitochondria of brain cells. *Se increased uptake of MeHg but not distribution to brain. *MeHg alone decreased GPx activity. Co-exposure prevented this.	Proha-ska & Ganther, 1977

One important aspect of their interactions is that mercury and selenium have a high binding affinity (Dyrssen & Wedborg, 1991); it is expected that the binding affinity of mercury for selenols (R-SeH) is greater than that for thiols (Canty *et al*., 1983). This affinity has a number of implications on the absorbance and distribution of both mercury and selenium in the brain.

Supporting this, exposure to MeHg has been correlated positively with total brain selenium levels. In monkeys (*Macaca fascicularis*) exposed to 50 μg/kg MeHgOH for 6–18 months, total brain selenium was positively correlated with total brain inorganic mercury (Bjorkman *et al*., 1995). Human brain tissue samples collected after death of humans exposed to environmental mercury concentrations through fish consumption, occupational exposure, or poisoning analysed for mercury, selenium, and mercury-selenium conjugates found a high proportion of the mercury present was found bound to selenium in Hg-Se complexes in both acute MeHg exposures and chronic low exposures (Korbas *et al*., 2010). This indicates that selenium does not facilitate excretion of MeHg or mercury from the brain. Moreover, this evidence suggests that the strong binding affinity of mercury with selenium allows them to form inert complexes that deposit in brain tissue. In addition, a number of studies have found that equimolar co-exposure of selenium is necessary to observe its full antagonism against MeHg toxicity, which has lead some researchers to suggest that complex-formation is part of the underlying mechanism (Khan & Wang, 2009). This provides further evidence that binding has a role in mercury-selenium interactions.

While some researchers have suggested that binding is responsible for selenium's antagonism, others have suggested that it is the root of MeHg neurotoxicity via selenium

deficiency (Ralston *et al*., 2012); however, this is unlikely to fully explain MeHg toxicity due to the many other toxic effects unrelated to selenium and the fact that selenium levels are highly regulated in the brain.

Finally, selenium might contribute to the decontamination process of mercury through altered distribution or excretion (Ohi *et al.,* 1975). Aside from complex formation, there is some evidence that this could also occur via selenium-mediated demethylation of MeHg. Khan and Wang (2010) reported that demethylation of MeHg occurred in the presence of seleno-amino acids via bis(methylmercuric)selenide intermediates; however, this study was not conducted in a biotic system. Supporting this idea, a previous study found evidence that MeHg could be demethylated using selenium-intermediates in dolphin liver (Palmisano *et al*., 1995). If demethylation of MeHg occurs after it has entered the brain (Friberg & Mottet, 1989), as has been shown to occur in astrocytes (Shapiro and Chan, 2008), this could decrease the ability of MeHg to depurate from the brain, as inorganic mercury does not readily cross the blood-brain barrier (Friberg & Mottet, 1989); however, were demethylation to occur within the rest of the body, this could prevent it from crossing the blood-brain barrier, increase excretion of Hg from the body, and decrease toxicity (Khan *et al*., 2009).

Aside from altering the toxicokinetics of MeHg, selenium and MeHg are related by their opposing effects on cellular redox function. While selenium is integral to several major antioxidation pathways, MeHg alters mitochondrial function and increases ROS. Studies have shown that co- or pre-exposure to selenium with MeHg yields a decrease in toxic effects on selenoenzyme activity and markers of oxidative stress (Roos *et al*., 2009; Branco

et al., 2012). Moreover, selenium deficiency has been shown to exacerbate these effects (Nishikido *et al*., 1987; Watanabe *et al*., 1999), suggesting that selenium is important in protecting against MeHg toxicity.

Based on the evidence, several hypotheses of the mechanism and significance of mercury-selenium interactions have been proposed. (1) Mercury-selenium binding decreases selenoenzyme activity and selenium supplementation restores enzyme activity and anti-oxidation capacity. (2) Selenols compete with thiols for mercury binding, preventing mercury from reaching its target, since MeHg has a greater binding affinity to selenols than to thiols. (3) Selenium causes mercury to re-distribute and excrete. (4) Selenium increases mercury demethylation. It is evident that selenium is important in MeHg neurotoxicity but further research is needed to clarify its roles and significance.

1.1.6. Therapeutic potential of selenium

There is no completely effective therapy for MeHg toxicity. In poisonings, chelators have been used to limited efficacy (Carvalho *et al.,* 2007; Mitka, 2008); however, there is no treatment for low-dose, chronic toxicity. Because of their extensive interactions, selenium has been proposed as a potential therapy for MeHg toxicity and several selenium-containing compounds have been examined. Originally, research focused on inorganic selenium compounds, such as sodium selenite and selenate, for their antagonism against MeHg toxicity. More recently, research has shifted to dietary and novel organic selenium compounds, such as the endogenous selenomethionine as well as novel organoselenium

compounds like ebselen and diphenyl diselenide (Table 1.1) (Farina *et al*., 2003; de Freitas *et al*., 2009; Roos *et al*., 2009; Glaser *et al*., 2014).

A recent addition to medical and pharmacological research has been to formulate medicines as nanoparticles. Their small size confers unique properties not found in bulk materials. Due to their size, they have unique properties that make them promising for medicine as a novel approach to drug delivery. They can increase delivery of a drug while reducing the effective dose, and potentially reducing side effects (Desai, 2012). Furthermore, they can have altered distributions in the body by crossing directly through membranes rather than relying on transporters. This could allow nanoparticles to cross the blood-brain barrier (Lockman *et al*., 2002), which is often a hindrance of drugs that target brain diseases.

To the best of our knowledge, there are no publications that examine the effects of selenium nanoparticles (SeNPs) on mercury toxicity. Only one study was found that examined interactions of selenium nanoparticles and mercury, which was performed in an abiotic experiment. The research examined the efficacy of SeNPs in trapping mercury vapour from fluorescent light bulbs and found that they had a higher absorbency than non-nanoparticle selenium (Johnson *et al.*, 2008). While this research was not related to biological systems or MeHg, it does set the precedent that SeNPs might have an application in mercury research.

The majority of SeNP research has examined them for their chemo-preventative and -therapeutic properties, where they have been shown to increase cell death and decrease cell proliferation in cancerous cell lines (Abdulah *et al*., 2005; Yang *et al*., 2012; Lopez-Heras *et*

al., 2014). In addition, several murine studies have shown that SeNPs are less toxic than other forms of selenium, while maintaining their therapeutic benefits (Zhang *et al*., 2005; Wang *et al.*, 2007; Zhang *et al*., 2008; Benko *et al*., 2012).

Based on the antagonism of selenium and existing research on SeNPs, SeNPs could offer greater therapeutic potential against MeHg neurotoxicity than traditional forms of selenium. Selenium levels are well regulated in the brain (Savaskan *et al*., 2003), which could make it difficult to target MeHg neurotoxicity using traditional sources of selenium. Using SeNPs could address this barrier to finding a therapy for MeHg-induced neurotoxicity and supply greater concentrations of selenium to the brain to interact with MeHg. As well, while traditional forms of selenium are required in equimolar concentrations with MeHg to observe full antagonism (Khan & Wang, 2009), SeNPs might be able to be used in lower concentrations while still showing a high level of antagonism with MeHg neurotoxicity. Finally, based on existing toxicology data, SeNPs could be used with less chance of toxic side effects than traditional forms of selenium.

Because MeHg is a global contaminant and potent neurotoxicant with no completely effective therapy, and anthropogenic emissions of MeHg continue today, despite treaties to cut emissions, it remains important to find a therapy for MeHg exposure. Based on the theoretical properties observed in many nanoparticles and the toxicology evidence in the literature and interactions between selenium and mercury, SeNPs provide a possibility in finding a therapy for MeHg exposure.

1.2. Thesis purpose

1.2.1. Rationale

The complete mechanism of MeHg neurotoxicity is not completely understood. In particular, research historically focused on high exposures that are not environmentally relevant and focus has shifted to sublethal environmentally relevant concentrations only, approximately, in the past decade (Farina *et al*., 2011b; Korbas, *et al*., 2011). Similarly, the understanding of the mechanism and significance of mercury-selenium interactions is incomplete and there studies have only begun recently to examine their interactions using environmentally relevant levels of MeHg. More research is required that examines MeHg neurotoxicity and interactions with selenium using sublethal, environmental levels to clarify their mechanisms.

In addition, there is no treatment for MeHg toxicity. This is a major concern, given the frequent exposure in fish-eating populations. Several inorganic and organic seleno-compounds have been examined for their therapeutic effects against methylmercury toxicity and show antagonism against MeHg toxicity (Farina *et al*., 2003; de Freitas *et al*., 2009; Roos *et al*., 2009; Glaser *et al*., 2014) and reformulating drugs as nanoparticles might improve drug delivery. To date, SeNPs have been researched as anti-cancer therapies. In the course of this research, several formations of SeNPs have been developed, including organic coatings. These coatings can be used to increase the activity as well as bioavailability and cellular uptake of SeNPs (Wu *et al*., 2012).

Selenium nanoparticles could have and application as a therapy for MeHg neurotoxicity. Using nanoparticles composed of a selenite core coated in a polysaccharide-protein complex (PSP) derived from *Pleurotus tuber regium* mushrooms to decrease agglomeration and increase cellular uptake (Wu *et al*., 2012), we aimed to determine whether co-exposure with MeHg could antagonise MeHg neurotoxicity.

1.2.2. Objectives

We have examined the potential of a novel PSP-coated selenium nanoparticle (Wu *et al*., 2012) as a therapy for sublethal MeHg neurotoxicity using environmentally relevant concentrations of MeHg using primary mouse cerebellar astrocyte cultures as a model.

(1) Determine the toxicity of PSP-coated selenium nanoparticles in cerebellar astrocytes compared to seleno-L-methionine.

(2) Compare the efficacy of PSP-coated selenium nanoparticle antagonism against methylmercury toxicity in cerebellar astrocytes with that of seleno-L-methionine.

(3) Compare the effect of PSP-coated selenium nanoparticles on methylmercury toxicokinetics in cerebellar astrocytes with that of seleno-L-methionine.

1.2.3. Hypotheses

Sublethal MeHg will have adverse effects on all cerebellar astrocytes and granule neurons and co-exposure of cell cultures to selenium and methylmercury will reduce the detrimental effects.

(1) The PSP-coated selenium nanoparticles will be more toxic to astrocytes than seleno-L-methionine.

(2) When co-exposed with methylmercury, PSP-coated selenium nanoparticles will reduce the effects of toxicity with greater efficiency than seleno-L-methionine at less than a 1:1 exposure ratio with MeHg.

(3) The PSP-coated selenium nanoparticles will have greater cellular uptake than seleno-L-methionine in astrocytes. Furthermore, they will decrease cellular uptake of MeHg more than seleno-L-methionine in astrocytes.

2. Methods

2.1. Ethics disclaimer

All animals were handled in accordance with the University of Ottawa animal ethics board and followed the protocol BL-270 approved by the University of Ottawa Animal Care Committee by personnel fully trained according to University of Ottawa and Canadian Council on Animal Care standards (Appendix A).

2.2. Cell culture

Primary cerebellar astrocytes were used as the model for this study, and were collected based on Marek *et al*. (2008) with some modifications. The primary cerebellar astrocytes were collected from post-natal BALB/C mice aged 4–6 days. Animals were handled under sterile conditions, animals were euthanised via decapitation and cerebella were isolated and collected. Isolated cerebella were placed in a sterile 15 mL centrifuge tube containing Hank's balanced salt solution (HBSS) (HyClone, USA) on ice during the procedure. Then, 0.25% trypsin (HyClone, USA) was added to a concentration of 100 µL per 5 mL, the cerebella were triturated 2–3 times and incubated for 30 min at 36ºC in a MACSmix tube rotator (Miltenyi Biotec, USA). Next, 100 µL per 5 mL characterised fetal bovine serum (FBS) (HyClone, USA) was added to inhibit the trypsin and cells were dissociated via trituration with a 5-mL sterile serological pipette (Fisher, USA). The

suspension was filtered through a 70-µm sterile nylon mesh strainer (Fisher, USA) via gravity and centrifuged at 1200 rpm for 5 min. The supernatant was discarded and the cell pellet re-suspended in astrocyte specific media (ASM), comprised of minimum essential media/Earle's balanced salt solution with 2.5 g/L glutamate (MEM/EBSS) (HyClone, USA) supplemented with 10% characterised FBS and 1% penicillin-streptomycin (HyClone, USA). Cells were plated in untreated sterile vent-cap polystyrene culture flasks (ThermoScientific Biolite) at a concentration of approximately 5–10 cerebella per 75 cm^2. A complete media change was conducted after 24 hr and every 3–4 days thereafter.

At approximately 90% confluence, cells were purified using the MACS anti-GLAST magnetic microbead purification system (Miltenyi Biotec, USA). GLAST is highly expressed in astroglial cells, and the anti-GLAST microbeads have been shown to be astrocyte specific, yielding 90-95% purity following the procedure (Jungblut *et al*., 2012). Under sterile conditions, the astrocytes were dissociated by washing with phosphate buffered saline (PBS)(HyClone, USA) and incubating for 5–10 min with 0.25% trypsin, then, FBS was added to inactivate the trypsin and cells were transferred to a 15 mL sterile polypropylene centrifuge tube (Fisher, USA) and spun for 5 min at 1200 rpm. Then, the supernatant was removed and cells were re-suspended in ice-cold purification buffer containing PBS supplemented with 2.5% bovine serum albumin (BSA) (Miltenyi Biotec, USA) and strained with a 40 µM sterile nylon mesh cell strainer via gravity to remove large clumps. Then, cells were centrifuged at 1200 rpm for 5 min, the supernatant was removed, and cells were re-suspended in 100 µL of purification buffer. 20 µL of cold anti-GLAST biotin was added to the cells and cells were incubated for 20 min at 4ºC, shaking every 3–5 min. After incubation, 1 mL ice-cold purification buffer was added to the cells, they were

centrifuged at 1200 rpm for 5 min, and the supernatant was removed. Cells were re-suspended in 100 µL of ice-cold purification buffer and 20 µL anti-biotin-microbeads were added. The cells were incubated for 15 min at 4ºC, shaking every 3–5 min. After incubation, 1 mL of ice-cold purification buffer was added to the cells, they were centrifuged at 1200 rpm for 5 min, and the supernatant was removed. Cells were re-suspended in 500 µL cold purification buffer and run through an LS purification column (Miltenyi Biotec, USA). After collection of purified cells, cells were re-plated with ASM in vent-cap untreated polystyrene culture flasks and grown until sufficient numbers were achieved, to no more than three passages.

Cells were dissociated as described above and re-plated in well plates for experimentation, using a haemocytometer to count cells and ensure consistent density among all experiments. Cells were allowed to adhere to the well plates for 24 hr and observed under a phase-contrast microscope before dosing to ensure sufficient viability.

2.3. Mercury and selenium exposure

Methylmercury chloride was purchased as a 1000 ppm aqueous solution (Alfa Aesar, USA), which was diluted to approximately 100 µM in MEM/EBSS (HyClone, USA) and filter sterilised using a sterile 0.2 µm PES syringe filter (VWR, USA). This solution was measured in duplicate using a MA-3000 (NIC, Japan) mercury analyser to verify the concentration. The measured concentration was used for further solution preparation calculations.

Seleno-L-methionine (SeMet) was purchased as a powder (Sigma Aldrich, USA) and a concentrated solution of approximately 5 mM was prepared in milli-q water and filter sterilised using a sterile 0.2 μM syringe filter (VWR, USA). The concentration was verified via inductively coupled plasma-mass spectrometry (ICP-MS) for total selenium and the measured concentration was used for all further calculations. A 173-μM solution was prepared in MEM/EBSS.

The PSP-coated SeNPs were obtained from a lab at a listed concentration of 1.069 mM. Subsequent measurement using ICP-MS for total selenium determined a lower concentration of total selenium of 320 μM and this concentration was used for all further concentration calculations. A 32-μM solution was prepared in MEM/EBSS. Before handling SeNPs, the solution was vortexed for 1 min to re-distribute the nanoparticles. Astrocyte specific media spiked with MeHg, SeMet, or SeNPs was prepared within 24 hours of dosing to ensure freshness.

For the cell viability assays, spiked solutions were made for each exposure group. All media was removed and pre-warmed spiked media was added to each well and exposed for 24 hr.

For the co-exposure assays, primary cerebellar astrocyte cultures were exposed to 0.5 or 1 μM MeHg and SeNPs or SeMet at concentration ratios of 1:1, 2:1, or 4:1 MeHg-to-selenium. For 0.5 μM MeHg, this was equivalent to 0.125, 0.25, or 0.5 μM selenium and for 1 μM MeHg, this was equivalent to 0.25, 0.5, or 1 μM selenium. In addition, controls of

MeHg-only and selenium-only exposure groups were included in the experiments. First, separate solutions of MeHg, SeNPs, and SeMet were prepared and mixed into the wells (Table 2.1). Then, all media was removed and un-spiked ASM or selenium-spiked was added and incubated for 2 hr. This allowed more selenium to be taken up into the cells to improve the likelihood of seeing cellular interactions between selenium and mercury, rather than them binding in media before being taken up by the cells (Frisk *et al*., 2000; Frisk *et al*., 2001). After 2 hr, MeHg solutions were added and cells incubated for 24 hr (Table 2.2). Figure 2.1 shows a schematic of this dosing regime.

Table 2.1: Preparation of the MeHg, SeNP, and SeMet spiked media for the co-exposure experiments.

Chemical	Required concentration* (μM)	Concentration multiplication factor**	Actual Concentration of spiking solutions (μM)
MeHg	0.5	2	1
		4	2
	1	2	2
		4	4
SeNPs	0.125	1	0.125
		2	0.25
	0.25	1	0.25
		2	0.5
	0.5	1	0.5
		2	1
	1	1	1
		2	2
SeMet	0.125	1	0.125
		2	0.25
	0.25	1	0.25
		2	0.5
	0.5	1	0.5
		2	1
	1	1	1
		2	2

* The concentration required for the astrocyte exposure groups.
** Spiking solution concentrations were multiplied to account for dilution when multiple solutions were mixed into well plates.

Table 2.2: The MeHg, SeNP, and SeMet exposure regime for the co-exposure experiments.

Step	Exposure Group	Solution (type)	Solution volume (% of total well volume)
1	Unexposed control	Unspiked media*	100
2	MeHg-only control	Unspiked media*	50
3	Selenium-only control	Respective 1x selenium**	100
4	Co-exposure	Respective 1x selenium**	50
5	Incubate 2 hr		
6	MeHg-only control	Respective 2x MeHg***	50
7	Co-exposure	Respective 2x selenium**	25
		Respective 4x MeHg***	25
8	Incubate 24 hr		

* Astrocyte specific media.
** Either SeNPs or SeMet at the specific concentration required for each exposure group.
*** MeHg at the specific concentration required for each exposure group.

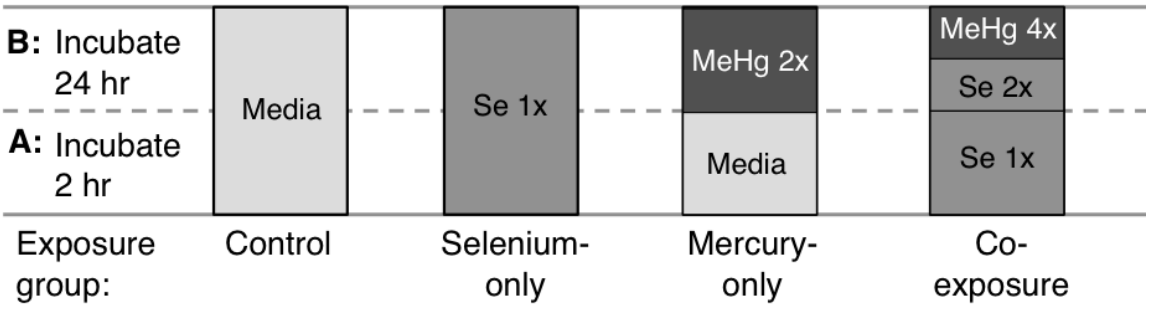

Figure 2.1: A schematic of the dosing procedure for co-exposures. First, old media was removed. (A) Media spiked with 1x-concentrated selenium (medium grey) or unspiked media (light grey) was added to exposure groups either containing or absent of selenium, respectively and incubated for 2 hr. (B) In co-exposure wells, media spiked with 2x-concentrated selenium was added, followed rapidly by 4x-concentrated MeHg (dark grey). In control wells containing only MeHg, 2x-concentrated MeHg was added. This was incubated for 24 hr.

2.4. Cell viability

Purified astrocytes were plated in transparent uncoated polystyrene 96-well plates (Corning, USA) at a density of 20 000 cells/well and allowed to adhere for 24 h. Then, a complete media change was performed and replaced with media spiked with either 0.5–10 µM MeHg, 8.2–1641.3 µM SeMet, or 0.16–32.7 µM SeNPs and incubated for 24 h at 37ºC and 5% CO_2. After 24 h, media was removed and all wells were rinsed with PBS.

For MeHg, SeNPs, and SeMet, tetrazolium dye (MTT) viability assays were conducted. The MTT solutions were prepared in advance by solubilising 5 mg/mL MTT in PBS and stored in the dark at –20ºC for up to two months. First, 120 µL of ASM containing a 5:1 dilution of MTT was added to each well and incubated for 3 hr at 37ºC and 5% CO_2. Media was removed carefully, so as not to disturb the formazan crystals precipitated during the incubation, and wells were allowed to dry completely for several minutes. Finally, 200 µL of dimethyl sulfoxide (DMSO) (Fisher, USA) was added per well and mixed to solubilise the formazan crystals. Wells containing no cells were included as experimental blanks. Absorbance was measured at 595 nm with a reference at 620 nm using a Tecan F200 Pro spectrometry plate reader.

For the data, average values from the control blanks were subtracted. Then, the average of the controls, the wells exposed to neither MeHg nor selenium, was determined and all values were converted to a percent of the average control. These values were used for the statistical analysis (see Section 2.9).

For MeHg exposure, a trypan blue assay was also performed. First, 45 µL 0.25% trypsin was added to each well and incubated for 5 min or until cells detached. Then, 5 µL of FBS was added to each well and cells were triturated with P200 pipette to form single cell suspensions. Finally, for each well, 25 µL of cell suspension was removed, mixed with 25 µL of trypan blue and loaded into both sides of a Neubauer haemocytometer. Total cells and dead cells, identified by their dark blue colour from absorption of trypan blue, were counted and recorded for all wells.

The data were collected as viable cells and dead cells for each replicate. These values were added for each replicate to yield total cells. For each replicate, viable cells were converted as a percent of total cells within that replicate. Then, the average percent viable cells determined for the control and all values were converted to a percent of the control. Similarly, the average of total cells counted was determined and all total cell counts were determined as a percent of the control. These values were used for further statistical analyses (see Section 2.9).

2.5. Cellular uptake of mercury and selenium

Purified astrocytes were plated in 6-well plates at a density of 125 000 cells per well and allowed to adhere for 24 hr. Then, a complete media change was performed and replaced with spiked media following the co-exposure methodology above and incubated for 24 hr at 37ºC and 5% CO_2. After 24 hr, media was removed and all wells were rinsed carefully three

times with PBS so as not to disturb the cells. Next, 200 µL of trypsin was added to each well and incubated to dissociate the cells. Cells were transferred to 1.5-mL polypropylene centrifuge tubes. All wells were washed once with 200 µL of PBS to maximise cell yield, which was transferred to their respective sample tube. Samples were frozen at –80ºC.

Next, samples were sonicated using a 90%-amplitude and 10-sec pulse to lyse the cells using a tabletop sonicator (Fisher Scientific model CL-18). Between samples, the sonicator arm was wiped clean with 90% ethanol and Kim wipes to prevent cross-contamination. From this, 50 µL of sample was loaded into the mercury analyser (MA-3000; NIC, Japan) for measurement of total mercury. The rest of the samples were re-frozen at –80ºC until further analysis.

The remainder of the samples were measured for total selenium. Samples were placed in 12×75 mm polystyrene round-bottom sample tubes (Falcon, USA) and diluted with Milli-Q water to 2 mL with 2% analytical grade nitric acid (Fisher, USA) for digestion. These tubes were nested in 15 mL centrifuge tubes (Fisher, USA) to fit in the ICP-MS auto-sampling apparatus. The use of the tube-within-a-tube set-up allowed for a lower dilution factor while maintaining sufficient sample height and volume to work with the ICP-MS auto-sampler. Finally, samples were measured for total selenium using ICP-MS.

For the total mercury analysis, sample blanks were below the detection limit, so these values were not subtracted from the rest of the samples. For the total selenium analysis, blanks were averaged and subtracted from sample values. For both, values were divided by number of cells in each sample, based on initial seeding cell count densities to yield the mass

of mercury and selenium per cell. These values were used for subsequent statistic analyses (see Section 2.9).

2.6. Cellular reactive oxidative species

Cellular ROS was measured using CellRox Green reagent (Life Technologies, USA). Primary cerebellar astrocytes were plated at a density of 20 000 cells/well in black, transparent-bottom 96-well plates (Brandplate, Germany). Cells were incubated for 24 hr at 37ºC and 5% CO_2. Then, media was removed and spiked media was added following the co-exposure methodology. After 24 hr, media was removed and cells were rinsed with pre-warmed PBS. CellRox Green loading solution was prepared fresh, within approximately 5 minutes of addition to cells, to a concentration of 10 µM in pre-warmed HBSS in the dark to prevent photo-oxidation. Then, 100 µL of loading solution was added to each well, with three additional wells for the negative control containing no dye and three additional wells for the H_2O_2 positive control. Based on an initial optimisation, cells were incubated for 60 min at 37ºC and 5% CO_2. The, cells were rinsed with pre-warmed HBSS and 50 µL of HBSS was added to each well. In the positive control wells, the HBSS contained 5 µL/mL H_2O_2. The plate was measured for fluorescence at 485/535 nm for excitation and emission.

After, measurements were normalised to protein content using BSA standards. Briefly, after measurement, all liquid was removed. Then, 25 µL of ice-cold 0.1% triton X-100 in PBS was added per well and incubated, shaken, for 2 min. From this, 15 µL per well was transferred to clear 96-well plates (Corning). As well, 10 µL of BSA standards of 0,

0.01, 0.1, 0.2, and 0.3 µg/mL were added in triplicate to empty wells and 5 µL of milli-Q water was added to standardise the volume. Finally, 200 µL Bradford reagent (Bio-Rad, USA) diluted 1:4 with Milli-Q water was added to each well and allowed to incubate for 5 min, agitated manually to ensure proper mixing of the reagent. The plate was read in a Tecan F200 pro spectrometry plate reader for absorbance at 595 nm.

The average fluorescence value of the control wells, exposed to neither mercury nor selenium, was calculated. All other values were determined as a percent of this average and used for subsequent analyses.

2.7. 2GSH/GSSG

The ratio of reduced-to-oxidised glutathione (2GSH/GSSG) assay was performed following Mailloux *et al*. (2014). Primary cerebellar astrocytes were plated at a density of 200 000 cells/well in 12-well plates (Corning, USA) and incubated for 24 hr at 37ºC and 5% CO_2 to adhere. Then, media was removed and replaced with spiked media following the co-exposure methodology. After 24 hr, spiked media was removed and cells were rinsed with PBS. For each well, PBS was removed and 150 µL of Optima water (Fisher, USA) was added. Cells were scraped with sterile cell scrapers (Fisher, USA). The liquid was transferred to a 1.5-mL polypropylene centrifuge tube (Diamed, Canada). Then, 75 µL of Optima HPLC-grade water (Fisher, USA) was added to the same well to collect remaining cells and transferred to the same tube, which was placed on ice while the rest of the samples were collected. Then, 25 µL of ice-cold 5% trace metal grade perchloric acid (Fisher, USA)

prepared in Optima water was added to each sample, yielding a final concentration of 0.5% perchloric acid and final sample volume of 250 µL and samples were incubated on ice for 10 min for digestion. After the digestion, sample were centrifuged at 10 000×*g* for 10 min at 4ºC. The supernatant was removed and frozen at –80ºC until analysis.

The sample analysis was conducted using high performance liquid chromatography (HPLC) with Agilent 1100 Series machine. Samples were run through an Agilent HPLC system with a Pursuit C_{18} column (150×4.6 mm, 5 µm; Agilent Technologies) at a flow rate of 1 mL/min. A mobile phase of 1% trifluoroacetic acid in water mixed at a 9:1 ratio with methanol was used. Reduced and oxidised glutathione solutions were prepared and used as standards.

Data were processed using Agilent ChemStation v. B.03.02. Reduced and oxidised GSH were determined by the area under the peak and quantified based on standard curves generated from GSH and GSSG standards run on the same day as the samples. Then, the ratio of 2GSH/GSSG was calculated and these ratios were used for further statistical analyses.

2.8. Enzyme activity

Primary cerebellar astrocytes were plated at a density of 20 000 cells per well in black transparent bottom 96-well plates (Brandplate, Germany). Cells were incubated for 24 hr at 37ºC and 5% CO_2 to adhere. Then, media was removed and spiked media was added

following the co-exposure methodology above. After 24 hr, media was removed and cells were rinsed with PBS. Then, 25 µL 0.1% saponin dissolved in potassium buffered saline was added to each well and incubated for 30 min at 4ºC. Cells were measured for GPx based on Paglia and Valentine (1967) or GR enzyme activity (Smith *et al*., 1988) based on NADPH fluorescence with modifications for measurements in 96-well plates based on a paper by Allen and colleagues (2001b) as described below. We used NADPH fluorescence instead of absorbance to reduce background absorbance caused by cellular proteins.

For GPx, on the same day as testing, GPx Reaction Buffer A and B were prepared. For a final volume Reaction Buffer A + B = 1 mL, Reaction Buffer A contained 21.1 µL 1M potassium phosphate monobasic, 28.9 µL 1M potassium phosphate dibasic, 10 µL 0.1 M tetrasodium ethylenediaminetetraacedic acid (EDTA), 100 µL 0.1M sodium azide, 100 µL 10 mM reduced glutathione, 256 µL µL milli-Q water, and 0.96 µL GR, while Reaction Buffer B contained 0.22 µL 30% hydrogen peroxide and 399.2 µL milli-Q water. In addition, Reaction Buffer A was prepared with water replacing the NADPH for six wells for sample blanks containing cells and without cells. As well, glutathione peroxidase (Sigma Aldrich, USA) standards of 0, 1, 5, 10, and 25 mU/mL were prepared. After the saponin incubation, 10 µL of the GPx standards were added to new wells in triplicate. Then, 75 µL of Reaction Buffer A was added to each well and allowed to incubate for 5 min. Reaction Buffer B was added within approximately 10 sec of beginning the fluorescence measurement using a Tecan F200 Pro plate spectrometer. Fluorescence using excitation and emission wavelengths of 350 (10) and 448 (8) nm was measured for 5 min at 15 sec intervals at 25ºC. Due to the rapid nature of the reaction, this process was repeated four wells at a time until all samples were complete.

For GR, on the same day as testing, GR Reaction Buffer A and B were prepared. For a final volume Reaction Buffer A + B = 1 mL, Reaction Buffer A contained 16.6 µL 1M potassium phosphate monobasic, 83.4 µL 1M potassium phosphate dibasic, 10 µL 0.1M tetrasodium EDTA, 440 µL milli-Q water, and 50 µL 2 mM NADPH, while Reaction buffer B contained 50 µL 20 mM GSSG and 350 µL milli-Q water. Volumes were increased as necessary for 125 µL Reaction Buffers A + B per well. In addition, Reaction Buffer A was prepared with water replacing the NADPH for six wells for sample blanks containing cells and without cells. As well, glutathione reductase (Sigma Aldrich, USA) standards of 0, 1, 5, 10, and 25 mU/mL were prepared. After the saponin incubation, 25 µL GR standards were added to new wells in triplicate. Then, 75 µL of Reaction Buffer A was added to each well and allowed to incubate for 5 min. Reaction Buffer B was added within approximately 10 sec of beginning the fluorescence measurement using a Tecan F200 Pro plate spectrometer. Fluorescence using excitation and emission wavelengths of 350 (10) and 448 (8) nm was measured for 5 min at 15 sec intervals at 25ºC. Due to the rapid nature of the reaction, this process was repeated four wells at a time until all samples were complete.

After, measurements were normalised to protein content using BSA standards. Briefly, after measurement, all liquid was removed. Then, 25 µL of ice-cold 0.1% triton X-100 in PBS was added per well and incubated, shaken, for 2 min. From this, 15 µL per well was transferred to clear 96-well plates (Corning). As well, 10 µL of BSA standards of 0, 0.01, 0.1, 0.2, and 0.3 µg/mL were added in triplicate to empty wells and 5 µL of milli-Q water was added to standardise the volume. Finally, 200 µL Bradford reagent (Bio-Rad, USA) diluted 1:4 with milli-Q water was added to each well and allowed to incubate for 5

min, agitated manually to ensure proper mixing of the reagent. The plate was read in a Tecan F200 pro spectrometry plate reader for absorbance at 595 nm.

Both GPx and GR activity were calculated based on the NADPH absorption coefficient according to equations from Northwest Life Science Specialties GPx and GR Assay manuals, respectively. Slopes and initial calculations were determined using Excel before exporting final values to JMP v.11 for final analyses. After determining enzyme activities, the values were normalised to the protein content of each sample.

For GPx, Equation (1) was used, where $mRate_s$ = -1000 × deltaA$_{340}$/min of sample, $mRate_b$ = -1000 × deltaA$_{340}$/min of blank, 2.99 = NADPH 340 nm millimolar absorption coefficient at 0.48 cm pathlength, V_{Rxn} = Volume of reaction mixture, V_s = volume of Sample, 2 = Correction for 2 mol GSH oxidised to 1 mol GSSG per mole NADPH oxidised, and df = sample dilution factor.

$$[GPx] = \frac{2(mRate_s - mRate_b) * V_{Rxn}}{2.99 * V_s} * df \qquad (1)$$

For GR, Equation (2) was used, where *–mrate* = 1000 * deltaA$_{340}$ of sample minus 1000 * deltaA$_{340}$ reaction blank, V_{Rxn} = volume of reaction mixture, V_s = volume of sample, *df* = dilution factor, and 2.99 = NADPH 340 nm millimolar absorption coefficient at 0.48 cm pathlength.

$$[GR] = \frac{(mRate * V_{Rxn})}{2.99 * V_S} * df \qquad (2)$$

2.9. Statistical analyses

Data were processed using Excel 2008 for Mac and statistics were performed using Jmp v.11. For all analyses, $p<0.05$ was considered statistically significant. Normality was tested using the Shapiro-Wilk test, and not all experiments passed the normality assumption, including: MeHg MTT and trypan blue, SeNP MTT, ROS, GR, and Hg uptake assays. Despite the low number of replicates and failing the assumption of normality, we conducted parametric analyses for all experiments based on a comparison of the results of parametric and non-parametric tests. Specifically, we compared the one-way ANOVAs with the Kruskal-Wallis test and the multi-way ANOVAs with both parametric and non-parametric regression analyses. We found that the results of the non-parametric analyses did not differ from those for the parametric tests for all experiments, suggesting that the failed assumptions and low replicates did not drastically alter the validity of the results.

For the cell viability assays, one-way analyses of variance (ANOVA) tests were performed. When significant, these were followed by a post-hoc Dunnett's test to compare with the control, the un-exposed group. For all co-exposure experiments, including the cell uptake, oxidative stress, and enzyme activity experiments, crossed-nested ANOVAs were performed MeHg concentration crossed with selenium concentration with selenium type nested. Due to the experimental set-up, only interactive effects were examined for significance, which were followed by a post-hoc Tukey's HSD test when significance was observed.

3. Results

3.1. Cell viability

Primary cerebellar astrocyte viability responded to 24-hr MeHg exposure in a dose-dependent manner, with decreasing viability for increasing concentrations of MeHg. Although we tested a limited range of MeHg, the trend suggests that it follows a traditional sigmoidal dose-response curve. The lowest observed effect level (LOEL) occurred at 2.5 and 5 μM MeHg for the MTT and trypan blue assays, respectively (Figs 3.1 and 3.2). Moreover, the total cells counted in the trypan blue assay were significantly lower than the control at 7.5 and 10 μM.

Similarly, primary cerebellar astrocyte viability responded to 24-hr SeNP and SeMet exposure in a dose-dependent fashion, with differences in the dose-response relationship observed between SeNPs and SeMet. After 24 hr exposure with either SeNPs or SeMet, the LOELs were 0.1634 and 1641.31 μM, respectively, based on the MTT assay (Fig. 3.3).

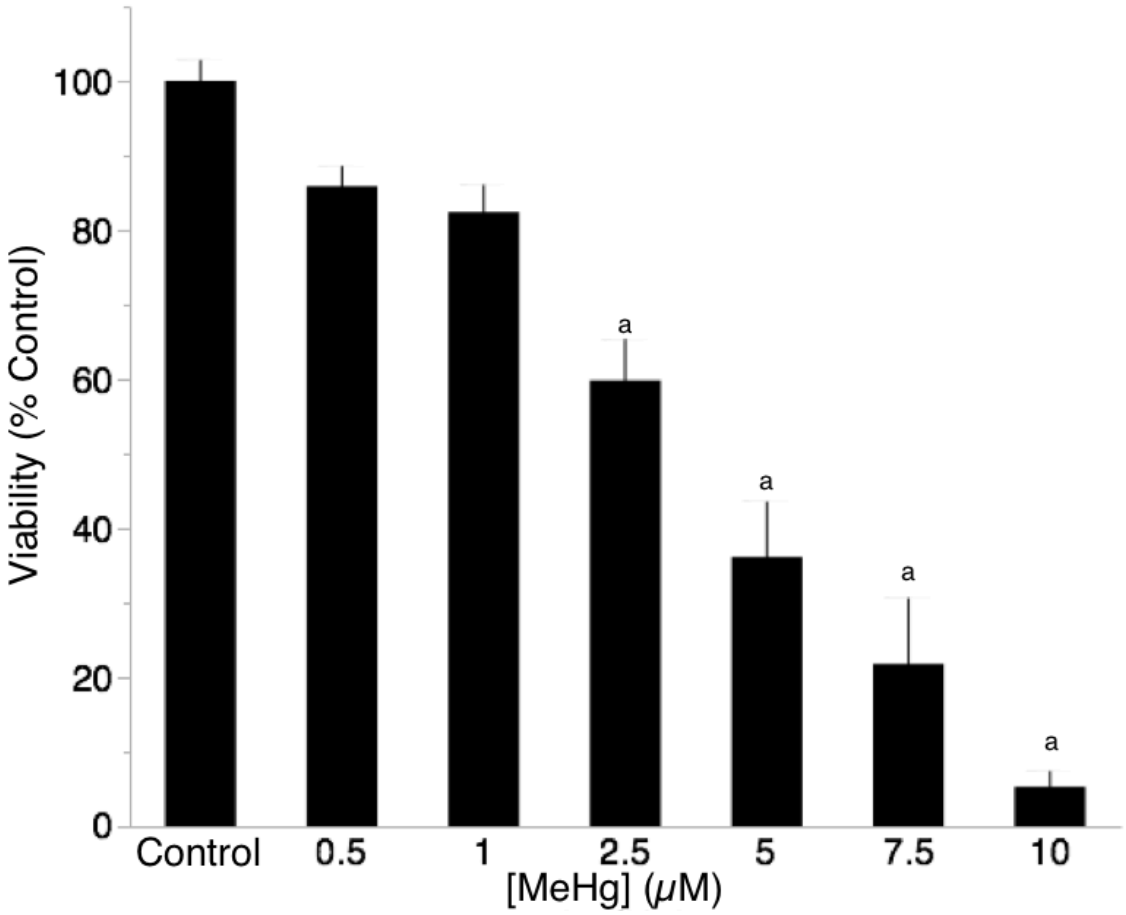

Figure 3.1: Viability of primary cerebellar astrocytes exposed to MeHg for 24 hr measured using the MTT viability assay. The effect of 24 hr MeHg exposure on primary cerebellar astrocyte viability. Response is based on the MTT assay. Results were analysed using 1-way anova followed by a post-hoc Dunnett's test. "a" indicates a significant difference from the control ($p<0.05$). Vertical lines represent standard error. n=4.

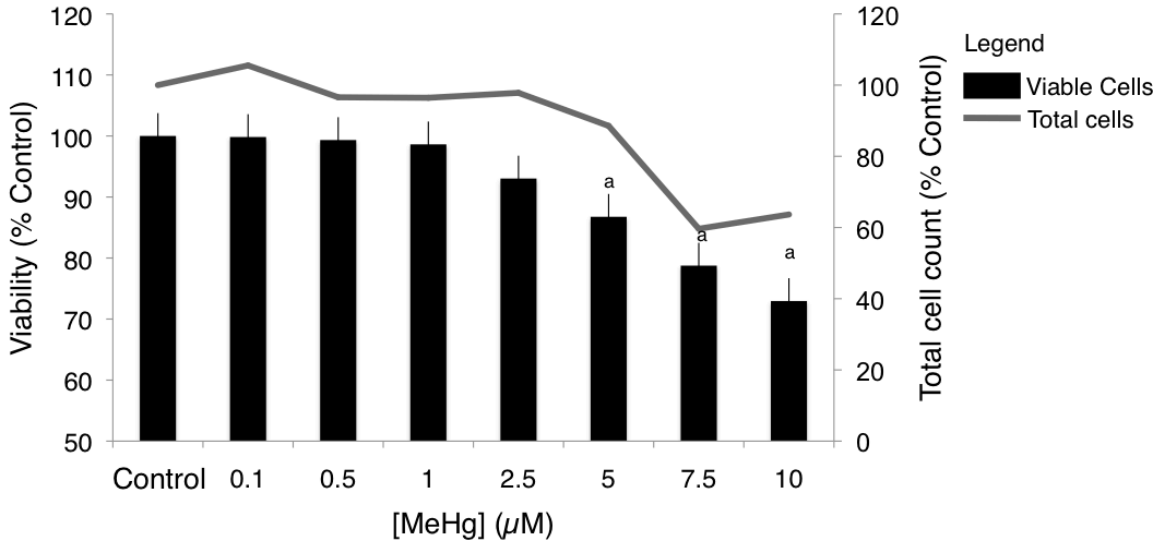

Figure 3.2: Viability of primary cerebellar astrocytes expose to MeHg for 24 hr measured using the trypan blue exclusion assay. The effect of 24 hr MeHg exposure on primary cerebellar astrocyte viability based on trypan blue exclusion assay as a ratio of dead to total cells counted (black bars). Grey line indicates total cell count. Results were analysed using 1-way ANOVA followed by a post-hoc Dunnett's test. "a" indicates a significant difference from the control ($p<0.05$). Vertical lines represent standard error. n=3.

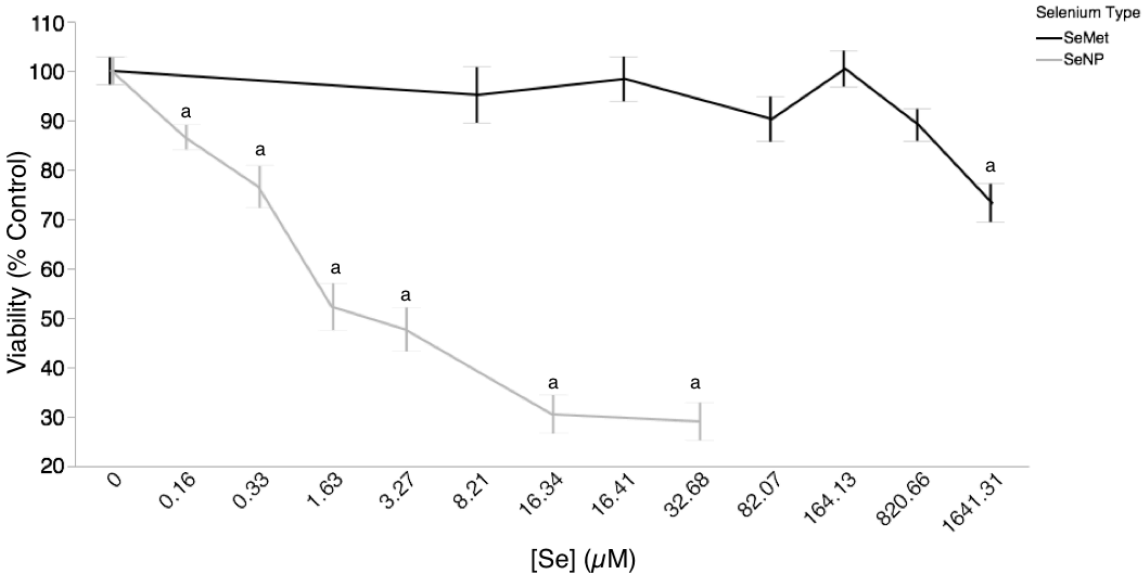

Figure 3.3: Viability of primary cerebellar astrocytes exposed to seleno-L-methionine or selenium nanoparticles for 24 hr measured using the MTT viability assay. The effect of 24 hr SeMet (black line) and SeNP (grey line) exposure to primary cerebellar astrocyte cultures based on the MTT assay. Results were analysed using 1-way ANOVA followed by a post-hoc Dunnett's test. "a" indicates a significant difference form the control ($p<0.05$). Vertical lines represent standard error. n=3. Horizontal axis not to scale.

3.2. Cellular uptake of mercury and selenium

Primary cerebellar astrocytes were measured for cellular uptake of total mercury after exposure to MeHg and SeNPs or SeMet. In groups exposed to no MeHg, no mercury was detected, indicating that the samples were insufficient to meet the detection limit of the MA-3000; however, this also indicates that there was no contamination or cross-contamination with mercury during the experiment. Cells exposed to 0.5 and 1 μM MeHg had increasingly significantly higher levels of total mercury. Co-exposure with SeMet had no significant effects at both levels of MeHg. Total mercury decreased significantly in a dose-dependent manner with co-exposure to increasing concentrations of SeNPs (Fig. 3.4).

Similarly, primary cerebellar astrocytes were measured for cellular uptake of total selenium after exposure to MeHg and SeNPs or SeMet. Cellular selenium increased significantly with increasing exposure to both SeNPs and SeMet. At the lower mono-exposures, 0.125–0.5 μM, SeMet was non-significantly higher than SeNPs, while at the highest mono-exposure, 1 μM, SeNPs were significantly higher than SeMet. Co-exposure with MeHg only significantly affected selenium uptake at the highest exposure of MeHg and SeNPs, 1 μM and 1 μM, resulting in lower cellular selenium (Fig. 3.5).

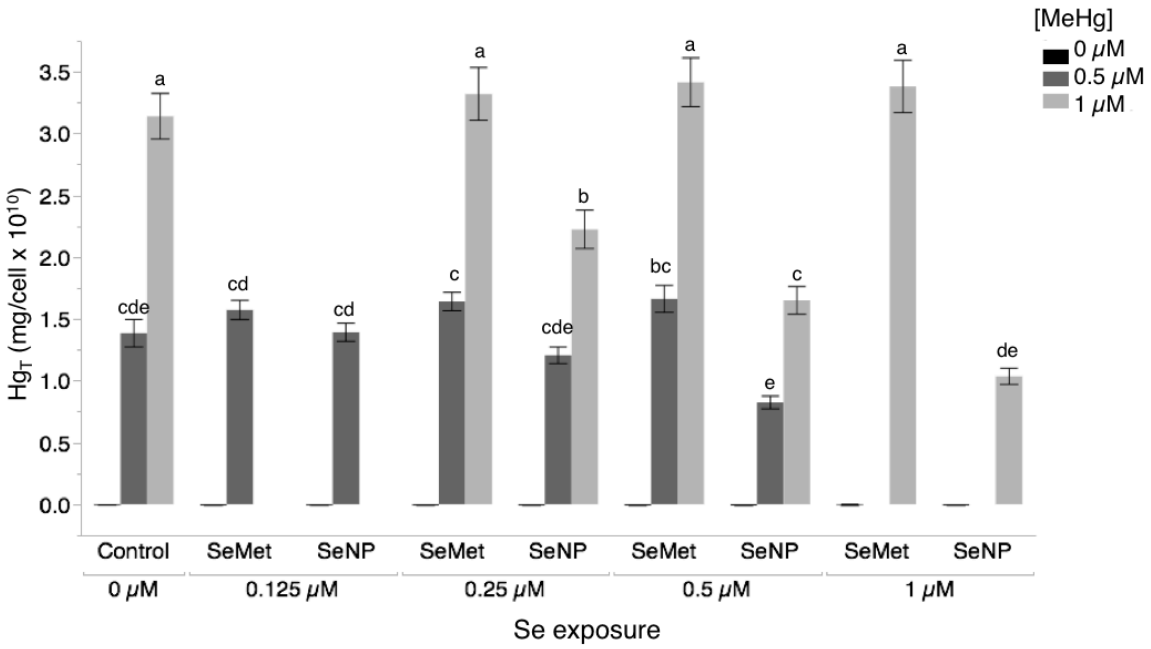

Figure 3.4: Cellular total mercury in primary cerebellar astrocytes exposed to MeHg and selenium nanoparticles or seleno-L-methionine for 24 hr. Cellular uptake of total mercury following co-exposure of MeHg and SeNPs or SeMet for 24 hr. Total mercury was measured using MA-3000 mercury analyser (Nippon Instruments, Japan). Results were analysed using ANOVA for MeHg and selenium, with selenium type nested, followed by a post-hoc Tukey's HSD test. Groups not connected by the same letter are significantly different ($p<0.05$). Unlabelled groups are not significantly different from the control 0 μM MeHg/0 μM Se. Vertical lines represent standard error.

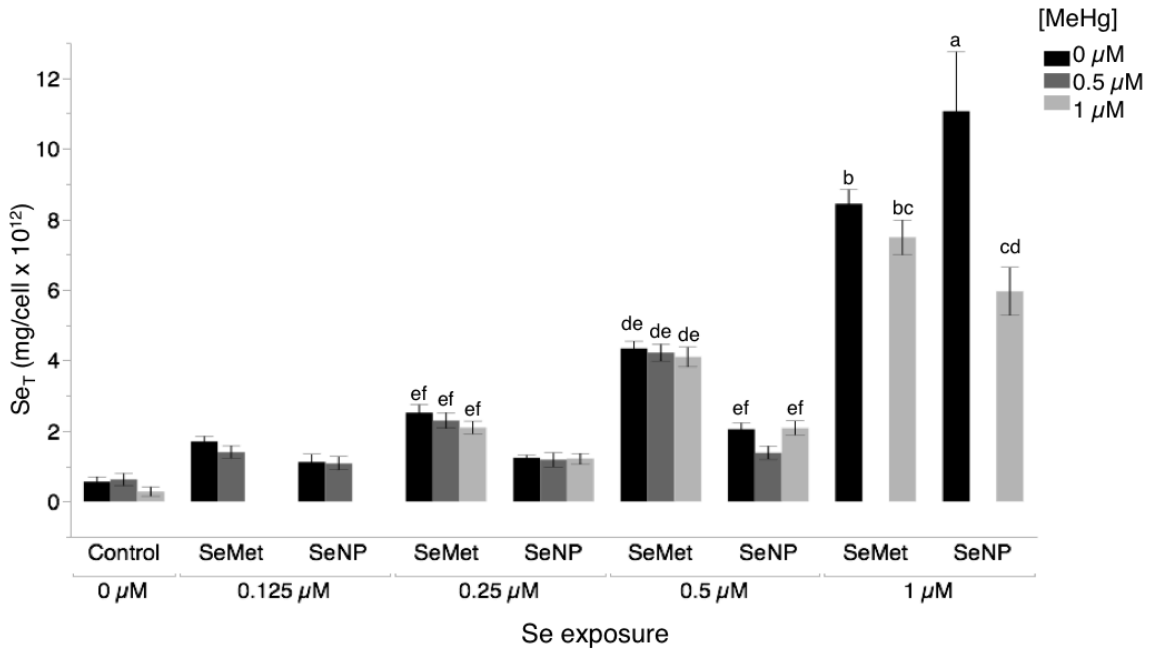

Figure 3.5: Cellular total selenium in primary cerebellar astrocytes exposed to MeHg and selenium nanoparticles or seleno-L-methionine for 24 hr. Cellular uptake of total selenium following co-exposure of MeHg and SeNPs or SeMet for 24 hr. Total selenium was measured using ICP-MS. Results were analysed using ANOVA for MeHg and selenium, with selenium type nested, followed by a post-hoc Tukey's HSD test. Groups not connected by the same letter are significantly different ($p<0.05$). Unlabelled groups are not significantly different from the control 0 μM MeHg/0 μM Se. Vertical lines represent standard error.

3.3. Oxidative stress

After co-exposure with MeHg and SeNPs or SeMet, primary cerebellar astrocytes exhibited significantly higher cellular ROS when exposed to 1 μM SeNP alone (Fig. 3.6). Furthermore, cellular ROS increased by SeNPs appeared to be dose-dependent. Methylmercury did not significantly increase ROS, although it appeared that ROS might correlated positively with MeHg concentration in the control groups. Finally, the 0.125 μM SeMet and 1 μM MeHg co-exposed with 0.5 μM SeNPs groups had significantly lower ROS. In all ROS experiments, the positive control using H_2O_2 induced higher ROS.

The ratio of 2GSH/GSSG was significantly higher in cells exposed to 0.5 μM SeNPs, which appeared to be dose-dependent from 0.125–0.5 μM. SeNPs co-exposed with MeHg did not have significantly higher ratio of 2GSH/GSSG. As well, 0.25 μM SeMet and 1 μM MeHg co-exposed with 0.5 μM SeMet resulted in a significantly lower ratio. No other groups had significant effects (Fig. 3.7).

There were no significant effects of the co-exposures on GR activity (Fig. 3.8) or GPx activity (Fig. 3.9).

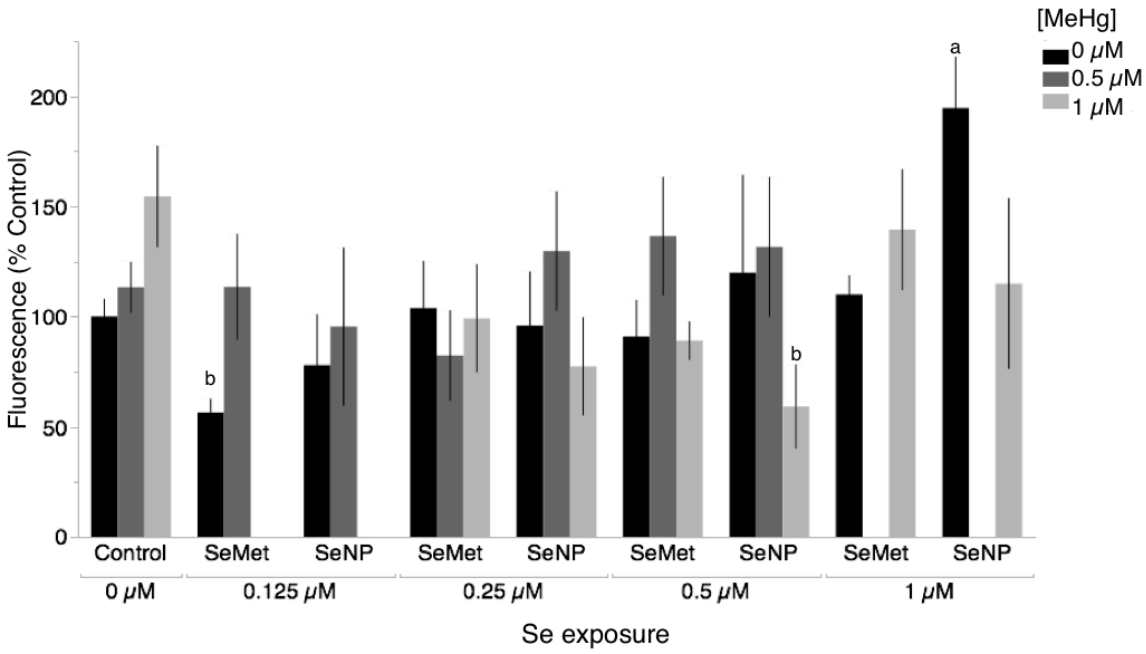

Figure 3.6: Cellular ROS in primary cerebellar astrocytes exposed to MeHg and selenium nanoparticles or seleno-L-methionine for 24 hr. Cellular reactive oxidative species production normalised to protein in primary cerebellar astrocytes exposed to 0 (black), 0.5 (dark grey), or 1 (light grey) μM MeHg and SeNPs or SeMet for 24 hr measured using CellRox Green fluorescence. Results were analysed using ANOVA for MeHg and selenium, with selenium type nested, followed by a post-hoc Tukey's HSD test. Significantly difference groups are labelled with a letter, a or b ($p<0.05$). n=3. All non-labelled groups belonged to both a and b. Vertical lines represent standard error.

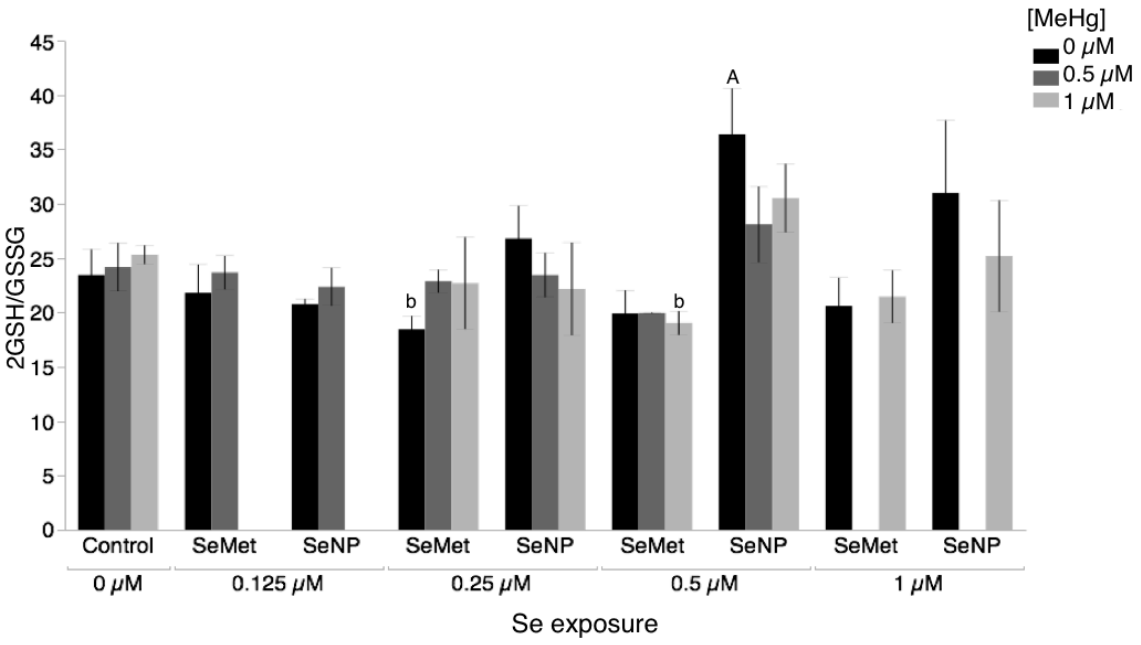

Figure 3.7: The ratio of reduced to oxidised glutathione (2GSH/GSSG) in primary cerebellar astrocytes exposed to MeHg and selenium nanoparticles or seleno-L-methionine for 24 hr. The cellular ratio of two reduced glutathione to oxidised glutathione in primary cerebellar astrocytes exposed to 0 (black), 0.5 (dark grey), or 1 (light grey) µM MeHg and SeNPs or SeMet for 24 hr measured using HPLC. Results were analysed using ANOVA for MeHg and selenium, with selenium type nested, followed by a post-hoc Tukey's HSD test. Significantly difference groups are labelled with a letter, a or b ($p<0.05$). n=3. All non-labelled groups belonged to both groups a and b. Vertical lines represent standard error.

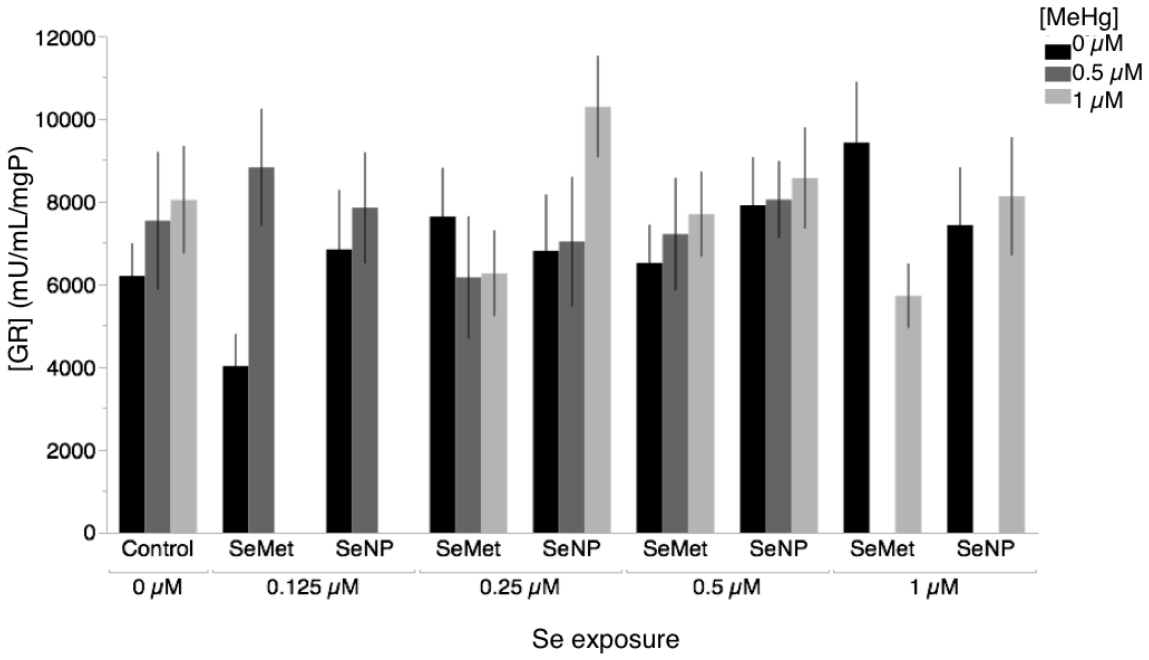

Figure 3.8: Glutathione reductase activity in primary cerebellar astrocytes exposed to MeHg and selenium nanoparticles or seleno-L-methionine for 24 hr. Cellular GR activity normalised to protein in primary cerebellar astrocyte cultures exposed to MeHg and SeNPs or SeMet for 24 hr measured using NADPH fluorescence. Results were analysed using ANOVA for MeHg and selenium, with selenium type nested. No significant differences were found ($p<0.05$). n=3. Vertical lines represent standard error.

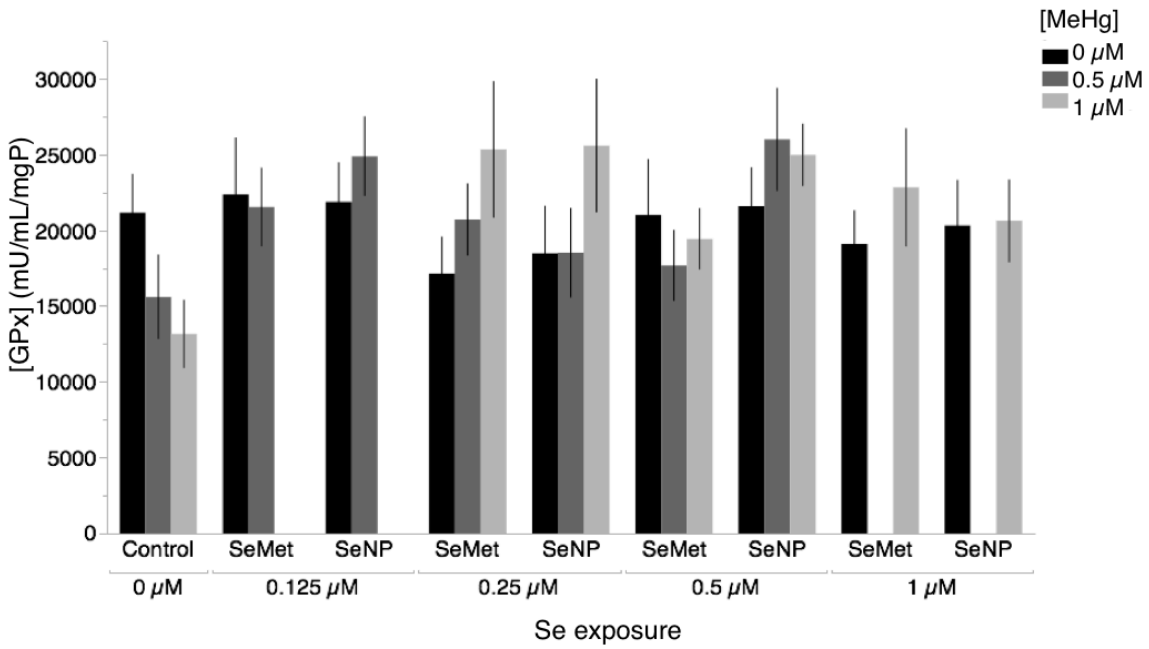

Figure 3.9: Glutathione peroxidase activity in primary cerebellar astrocytes exposed to MeHg and selenium nanoparticles or seleno-L-methionine for 24 hr. Cellular GPx activity normalised to protein in primary cerebellar astrocyte cultures exposed to MeHg and SeNPs or SeMet for 24 hr measured using NADPH fluorescence. Results were analysed using ANOVA for MeHg and selenium, with selenium type nested. No significant differences were found ($p<0.05$). n=3. Vertical lines represent standard error.

4. Discussion

We found that MeHg was toxic to primary cerebellar astrocytes, with LOELs of 2.5 and 5 μM using MTT and trypan blue assays, respectively, which were in general agreement with the literature. In one study, the LC_{50} of 24 hr MeHg exposure in primary human astrocytes was 8.1 μM, while that for a SH-SY5Y neural cell line and primary neurons were 6.9 and 6.5 μM, respectively (Sanfeliu *et al*., 2001). Based on the MTT assay results, we found an EC_{50} of 3.50 μM for MeHg, which was similar to this study. Methylmercury was found to have a LOEL of 0.5 μM MeHg in SH-SY5Y neural cells exposed for 24 hr measured with the CellTiter-Blue assay and 0.5 μM based on cell apoptosis (Franco *et al.* 2009). Given that Sanfeliu *et al*., (2001) found that the neural cell line was slightly more sensitive than primary astrocytes, we also consider this to support our results. Kaur *et al.* (2006) found that primary cerebellar astrocytes had significantly lower viability based on the MTT assay at 1 μM after 60 min incubation with MeHg, but not after 30 min, indicating greater sensitivity in their experiment than in this experiment, where 1 μM showed no significant difference even after 24 hr. Conversely, several studies have found much less sensitivity in astrocytes than we found. Ni *et al.* (2011) found no significant difference in primary rat astrocyte viability using an MTT and LDH assays up to 5 μM after 6 hr exposure, although this could be due to the shorter incubation period than in our study. Finally, Morken *et al*. (2005) found an EC_{50} of 39.5 μM in primary mouse cerebellar astrocytes and 33.0 μM in cortical astrocytes, while 2.2 μM for cerebellar neurons. Examination of the methods does not explain this discrepancy.

Cell viability for MeHg was tested to determine sublethal concentrations of MeHg for subsequent experiments. Concentrations of ≤1 and ≤2.5 μM exhibited no significant difference from the control based on the MTT and trypan blue assays, respectively. Moreover, we wanted to conduct the co-exposure experiments using environmentally relevant exposures to humans. Based on a study by Korbas *et al*., (2011), MeHg in human brain tissue of fish and non-fish eaters who had died of natural causes was measured between 0.2–1.4 μM. Therefore, we chose concentrations of 0.5 and 1 μM for the co-exposure experiments, which were both sublethal based on both viability experiments and environmentally relevant. Furthermore, initial optimisations (results not shown) of the cellular ROS and enzyme activity assays using low doses of MeHg suggested that these would yield sublethal effects. While such low concentrations of MeHg may be more relevant to real-world exposures, using low concentrations of MeHg can also make experimentation more difficult, as the effects can be more subtle, requiring more sensitive analytical procedures.

The trypan blue assay results were based on the ratio of dead cells to total cells counted. At the highest concentrations, 7.5 and 10 μM MeHg, total cell count was significantly lower than at the control, likely reflecting dead cells that had dissociated from the well plates and washed away during the procedure. However, they were not taken into account in the calculation because there was no significant difference at lower concentrations and would likely have not had a large effect on the LOEL values. Since the purpose of this experiment was only to determine the LOEL and sublethal values of MeHg, we consider the current analyses to be sufficient.

The LOEL values for primary cerebellar astrocytes exposed to SeMet and SeNPs were 1641.31 and 0.16 μM, respectively. Results on SeMet and SeNP toxicity in cell cultures vary in the literature. No studies were found that examined SeMet toxicity in brain cell cultures. Several other studies roughly confirmed our SeMet toxicity results. One study conducted on BALB/c MK-2 epidermal cell line exposed to 5 or 10 μg/mL (25.5 or 50 mM) SeMet for 24 hr resulted in 52 and 54% attached cells compared to the control, respectively, but no detached cells (Stewart *et al*., 1999). Another study using the HepG2 liver cell line exposed to SeMet for 24, 48, and 72 hr found no significant toxicity up to 1 mM (Hoefig *et al*., 2011). While these studies use different dosing regimes and are not completely analogous to our results, they indicate similar trends as our observations that SeMet has a relatively low toxicity.

Conversely, some studies have found greater toxicity for SeMet than we observed. In a study using R1.1 and K-562 cell lines exposed to SeMet for 72 hours, cell growth was inhibited by 50% between 40–160 μM in both cell lines based on a cell counting assay (Kajander *et al*., 1991). As well, an experiment using four colon cancer cell lines found no significant decrease in cell viability after 24 hr with SeMet exposure up to 100 μM; however, decreases were observed after 48 and 72 hr incubation with 50 and 100 μM SeMet (Goal *et al*., 2006). The higher toxicities observed in these experiments could be explained in part by the longer duration of exposure, but also due to differences between the cell lines and the primary astrocytes used in this study.

Similarly, no studies have examined SeNP toxicity in brain cells. However, studies have been conducted on other cell lines. Some studies have found that SeNPs are more toxic to cancerous cell lines than non-cancerous cell lines. However, our non-cancerous primary cerebellar astrocyte toxicity results were more in line with toxicity in cancerous cell lines. A previous study using the same formulation and source of PSP-coated SeNPs in examining their anti-cancer activity found that they had a 24 hr LOEL of 3 μM and IC_{50} of 3.7 μM on MCF-7 cancer cell growth based on the MTT assay, while a non-cancerous fibroblast cell line Hs68 had a 24 hr LOEL of 15 μM viability and viability did not decrease more than 50% up to exposure of 120 μM (Wu *et al*., 2012). In this study, the same PSP-coated SeNPs had an EC_{50} of 2.0 μM. One explanation of the higher sensitivity observed in this study is that either primary cells or astrocytes are more sensitive to these PSP-coated nanoparticles than either of the cell lines used in the previous study. There is evidence that some neurons are sensitive to metallic nanoparticles (Scott, 2012), which might also be the case for astrocytes. Another explanation is that, in our initial analysis of total selenium of the SeNP stock solution using ICP-MS, we determined total selenium to be about 30% that of the stated concentration. It is possible that the previous study used had higher stated values than actual values for their selenium, therefore inflating the LOEL and IC_{50} values.

In support of the previous study, an experiment using on four cancer cell lines and one non-cancer cell line, Hs68, exposed to polysaccharide-coated SeNPs for 72 hr found IC_{50} values ranging from 3–14.1 and 67.9 μM, respectively, based on an MTT assay (Chen *et al*., 2008). Another study using HepG2 liver cancer cell line and HK-2 non-cancerous kidney cell line found no significant decrease in viability up to 40 μM SeNPs with ATP surface decoration for 24 hr on the non-cancerous cells, but IC_{50} of 5~10 μM for the cancerous cells

(Zhang *et al*., 2012). Explanations for the differences in toxicity between these studies and ours could be differences in coatings, differences among cell lines and primary cells, or differences among cell types.

Since this experiment is the first to examine the effects of SeNPs on MeHg toxicity, it would have been optimal to include a control containing only the PSPs used for the nanoparticle coating to determine if they altered the effects of the SeNPs; however, this coating was formed from a specific fraction of *Pleurotubus regimens* mushroom extract by another laboratory (Zhang *et al*., 2001; Wu *et al*., 2012) and it would have been infeasible to have attempted to make and include in these experiments. In addition, selenium might dissociate from the nanoparticle core into solution; however, it is unknown how much this occurred and how much this could have contributed to the overall effects of the SeNPs. Ideally, this would have been determined and included as a control. Since it may be possible for nanoparticles to cross the blood-brain barrier (Lockman *et al*., 2002), further studies on neurotoxicity of SeNPs is necessary to clarify whether SeNPs in general, and with specific formulations and coatings are neurotoxic, regardless of their medical application.

Our results do not explain why the SeNPs were more toxic than SeMet to the cerebellar astrocytes, although in examining the literature, there are several possibilities. In general, nanoparticle formulations can allow for increased uptake (Verma & Stellacci, 2010). However, since the SeNPs used in this study did not significantly increase cellular selenium until 1 μM, while SeMet increased cellular selenium at lower concentrations, increased cellular uptake does not explain the higher toxicity of SeNPs than SeMet below 1 μM. Nanoparticles can also alter distribution. If distribution is altered in sub-cellular

compartments, toxicity could be altered if deposition is higher in compartments that are targets of toxicity, even if total cellular levels are not significantly different than non-nanoparticles. Further experiments testing selenium levels in sub-cellular compartments are necessary to clarify this.

In addition, brain cells are sensitive to oxidative stress, likely due to the high energy demand of these cells (Lin & Beal, 2006). As well, nanoparticles can induce oxidative stress (Xia *et al*., 2009; Manke *et al.*, 2013). This could make brain cells more sensitive to nanoparticles than other cell types. Furthermore, while the mechanisms of selenium toxicity are not well known, oxidative stress is likely involved. It has been suggested that selenium can interact with thiol reactive groups in enzymes required for cellular respiration, leading to mitochondrial dysfunction (ATSDR, 2003). This supports that the toxicity of SeNPs in astrocytes could have occurred via a mechanism related to oxidative stress.

Converse to our findings, several *in vivo* studies have found that SeNPs exhibit lower toxicity than non-nano selenium (Benko *et al*., 2012; Shakibaie *et al*., 2013), although this can depend greatly on nanoparticle size and composition. Our results did not mirror these observations, which could be attributed to differences in toxicokinetics, especially distribution, between *in vivo* versus *in vitro* studies. Moreover, it has been suggested that some neural cells might be sensitive to nanoparticle toxicity, which could explain their high toxicity in this study (Scott, 2012). However, further research using this particular composition of nanoparticle is necessary to clarify this.

Finally, it is unknown if the effects of the SeNPs based on the MTT assay are based on mitochondrial dysfunction or on increased cell death. Based on intended experiments, the supply of SeNPs was limited. Due to the large range in doses, this experiment used the greatest amount of nanoparticles and it was not possible to conducted additional experiments. For future experiments, it would be valuable to conduct additional viability tests, since the cellular ROS and 2GSH/GSSG experiments suggest that SeNPs induce ROS production, which could influence MTT assay results. This could also help clarify if SeNP toxicity was due to oxidative stress.

Methylmercury uptake was not affected significantly by co-exposure with SeMet, but decreased significantly with increasing concentrations of SeNPs. While co-exposure of 0.5 μM MeHg with SeMet did not have any significant differences from the 0.5 μM MeHg control, increasing concentrations of SeMet were connected to groups of higher concentrations, indicating a slight non-significant increasing trend of MeHg uptake with increasing SeMet. Our original hypothesis was that SeMet would significantly decrease MeHg uptake at equimolar co-exposures and that SeNPs would also significantly decrease MeHg uptake, but at higher ratios of MeHg:Se. This was based on observations that equimolar concentrations of selenium to mercury are required for the full antagonism of selenium to occur (Khan & Wang, 2009), and with observations that nanoparticles can have higher availability and uptake (Machado *et al*., 2010) and exert greater effects at lower concentrations (De Jong & Borm, 2008). Since one hypothesis is that selenium binds with mercury, it was expected that SeMet would have significant effects on MeHg uptake at 0.5 μM when co-exposed with 0.5 μM SeMet and 1 μM when co-exposed with 1 μM SeMet; however, SeMet did not have significant effects on MeHg uptake. The SeNPs significantly

decreased uptake of MeHg, in a dose dependent manner. Similarly, MeHg significantly decreased uptake of SeNPs at their highest level, indicating that SeNPs had greater ability to interact with MeHg. Based on results from an inorganic study examining SeNPs as a sorbent for inorganic Hg, it was suggested that Hg was able to bind to sub-surface Se in the nanoparticles (Johnson *et al*., 2008). It is possible that the MeHg interacted similarly with the SeNPs similarly in this experiment, either in the extracellular matrix preventing uptake, or within cells, increasing excretion.

In this study, cellular ROS, 2GSH/GSSG, and GR and GPx activity were used to observe the effects of MeHg on cellular oxidative stress. Based on the ROS and 2GSH/GSSG experiments, MeHg had no significant influence on the oxidative state of the astrocytes after 24 hr, despite a dose-related trend in increasing ROS with increasing MeHg in the controls. This contradicted our hypothesis that MeHg would significantly increase oxidative stress. There was some limited and conflicting evidence that exposure to SeMet decreased cellular oxidative stress alone and co-exposed with MeHg, which partially validated our hypothesis that co-exposure with SeMet would prevent or ameliorate MeHg-induced ROS production, although the results are too variable to state this with certainty. In general, previous studies have found that sublethal MeHg increases cellular ROS (Ni *et al*., 2011; Kaur *et al*., 2007) and co-exposure with selenium prevents or ameliorates this (Roos *et al*., 2009; Yamashita *et al*., 2013). Given that ROS and MeHg appeared to be correlated, it is possible that the concentrations used in this study were too low to observe significant effects and since a significant increase in ROS was not observed with MeHg alone, there was no effect for the co-exposure with selenium to antagonise.

The LOELs of the MTT and trypan blue viability assays support this, as the former was 2.5 μM while the latter was 5 μM. We interpreted these results to in relation to viability. However, the MTT assay can also be a measure of mitochondria function, as it relies on mitochondrial enzyme activity to complete the assay. Since no effects were observed until 2.5 μM, it is possible that using concentrations of 0.5 and 1 μM were too low to produce significantly higher ROS after 24 hr exposure. Given this, the trypan blue assay might have been more indicative of cell viability rather than the MTT assay, which could have been more indicative of mitochondrial function and oxidative stress, especially at the lower exposure levels. Another possibility is that, by measuring ROS after 24 hr, the maximum ROS production event was missed. Induction of ROS can occur rapidly. Some studies have examined acute MeHg exposure and detected elevated ROS after only 30 min (Shanker *et al*., 2004). Although it was not the intent of this study to examine acute effects of MeHg, the primary ROS event after initial exposure to MeHg could have occurred earlier. A follow-up experiment measuring downstream effects of ROS, such as TBARS or 4-hydroxynonenal, by-products of lipid peroxidation, could confirm this possibility.

Results from the ROS assay indicated that SeNPs significantly increased cellular oxidative stress alone; however, no significant increases were observed with co-exposure to SeNPs. This contradicted our hypothesis. Given that MeHg and selenium have a strong binding affinity that has been attributed to the antagonism of selenium against MeHg toxicity, it is likely that this binding caused MeHg to antagonise the oxidative stress induced by SeNPs.

Selenium nanoparticles alone significantly increased the ratio of 2GSH/GSSG at 0.5 μM, and this increase appeared to follow a dose-dependent trend up to 0.5 μM, after which the ratio decreased. This is not in agreement with the existing literature that SeNPs are less toxic than non-nano selenium and mostly toxic to cancerous, rather than non-cancerous cells. Normally, under oxidative stress, 2GSH/GSSG is expected to decrease. However, according to the oxidative stress paradigm, low exposures might initially trigger up-regulation of antioxidants such as GSH, acting as a compensatory mechanism (Xia *et al*., 2006). In examining the raw data, it appeared that the increase in 2GSH/GSSG was due to increase in absolute GSH rather than a decrease in GSSG, supporting the possibility that low exposure SeNP-induced oxidative stress triggered compensatory GSH production, further examination of SeNPs at higher doses could clarify these trends.

Although there were no significant differences in GPx and GR activity among exposure groups, there was a trend in decreasing GPx activity with increasing MeHg exposure that appeared to be attenuated with SeMet and SeNP exposure. There is evidence in the literature that MeHg decreases GPx activity (Franco *et al*., 2009), possibly because it is a selenoenzyme. For example, Franco *et al*., (2009) found a significant decrease in GPx activity at 1 μM MeHg, by about 70% of control, but not at 0.5 μM in SH-SY neural cells. Further research is necessary to clarify potential interactions between SeNPs and MeHg on GPx activity using a more sensitive method or by verification of protein content with Western blot.

Overall, our results indicated that SeNPs were more toxic than SeMet and that they had greater effects on cellular oxidative stress than MeHg. As well, there were greater

interactive effects between SeNPs and MeHg on cell uptake than between SeMet and MeHg. Despite these interactions, there is not strong evidence that SeNPs would make an effective therapy against MeHg neurotoxicity at the exposures and formulation used; however, more research is necessary to clarify this.

5. Conclusions

We researched the potential of selenium nanoparticles in antagonising methylmercury neurotoxicity compared to selenomethionine using primary astrocyte cell cultures and examining outcomes related to oxidative stress. However, we found that SeNPs were more toxic than SeMet in primary cerebellar astrocytes. Increasing SeNPs significantly decreased MeHg cellular uptake and MeHg significantly decreased uptake of SeNPs at the highest concentration. Finally, SeNPs alone produced significantly higher reactive oxidative species and decreased the ratio of reduced-to-oxidised glutathione, but MeHg, SeMet, and co-exposures did not. There were no significant effects on glutathione peroxidase or reductase activity. Our results suggest that SeNPs are more toxic than MeHg in cerebellar astrocytes and that they may not be suitable as a therapy at the doses and formulation used in this experiment. In addition, this could provide evidence of nanoparticle toxicity, suggesting caution in using SeNPs as therapies in other medical applications.

5.1. Future directions

Further experiments are needed to more fully explain the toxicity of the selenium nanoparticles observed in this study, as well as their interaction with methylmercury. Similarly, since toxicity was observed with these nanoparticles, additional work should explore the potential of SeNPs as a therapy for MeHg toxicity using lower doses and different formulations. Since interactions between neurons and astrocytes are important in

MeHg neurotoxicity, similar interactions between selenium and MeHg should be explored in neuron cultures and co-cultures of neurons and astrocytes. Finally, some of the results in this study should be clarified using more sensitive techniques, including the enzyme assays, which could be validated with Western blot analyses.

References

Agency for Toxic Substances and Disease Registry (ATSDSR) (2003). Toxicological Profile for Selenium. *US Department of Health and Human Services, Public Health Services: Atlanta, GA, USA*

Allen, J. W., Shanker, G., & Aschner, M. (2001a). Methylmercury inhibits the in vitro uptake of the glutathione precursor, cystine, in astrocytes, but not in neurons. *Brain research*, *894*(1): 131–40.

Allen, S., Shea, J. M., Felmet, T., Gadra, J., & Dehn P. F. (2001b). A kinetic microassay for glutathione in cells plated on 96-well microtiter plates. *Methods in Cell Science 22*: 305–312.

Allen, J. W., Shanker, G., Tan, K. H., & Aschner, M. (2002). The consequences of methylmercury exposure on interactive functions between astrocytes and neurons. *Neurotoxicology*, *23*(6), 755–9.

Arakawa, S., Bach, R.D. & Kimura, T. (1980). Kinetic study of the interaction of methylmercury with the Fe2S2(SR)4 cluster of adrenodoxin. *Journal of the American Chemical Society*, *102*: 6847–6849.

Arnér, E. S. J. (2009). Focus on mammalian thioredoxin reductases--important selenoproteins with versatile functions. *Biochimica et Biophysica Acta*, *1790*(6): 495–526.

Aschner, M. & Aschner J. L. (1990). Mercury Neurotoxicity: Mechanisms of Blood-Brain Barrier Transport. *Neuroscience & Biobehavioural Reviews*, *14*: 169–176.

Aschner, M., Eberle, N. B., Goderie, S., & Kimelberg, H. K. (1990). Methylmercury uptake in rat primary astrocyte cultures: the role of the neutral amino acid transport system. *Brain Research*, 521: 221–228.

Aschner, M., Yao, C. P., Allen, J. W., & Tan, K. H. (2000). Methylmercury alters glutamate transport in astrocytes. *Neurochemistry International*, 37(2-3), 199–206.

Bachrach, S. M., Demoin, D. W., Luk, M., & Mill, J. V. Jr. (2004). Nucleophilic attack at selenium in diselenides and selenosulfides. A computational study. *Journal of Physical Chemistry*, *108*(18): 4040–4046.

Bal-Price, A., & Brown, G. C. (2001). Inflammatory neurodegeneration mediated by nitric oxide from activated glia-inhibiting neuronal respiration, causing glutamate release and excitotoxicity. *The Journal of Neuroscience*, *21*(17): 6480–91.

Basu, N., Scheuhammer, A. M., Evans, R. D., O'Brien, M., & Chan, H. M. (2007). Cholinesterase and monoamine oxidase activity in relation to mercury levels in the cerebral cortex of wild river otters. *Human & Experimental Toxicology*, *26*(3): 213–20.

Behne, D. & Kyriakopoulos, A. (2001). Mammalian selenium-containing proteins. *Annual Reviews of Nutrition*, *21*: 453–473.

Benko, I., Nagy, G., Tanczos, B., Ungvari, E., Sztrik, A., Eszenyi, P., Prokisch, J., & Banfalvi, G. (2012). Subacute toxicology of nano-selenium compared to other selenium species in mice. *Environmental Toxicology and Chemistry*, *31*(12): 2812–2820.

Berg, K., Puntervoll, P., Valdersnes, S., & Goksøyr, A. (2010). Responses in the brain proteome of Atlantic cod (*Gadus morhua*) exposed to methylmercury. *Aquatic Toxicology*, *100*(1): 51–65.

Björkman, L., Mottet, K., Nylander, M., Vahter, M., Lind, B., & Friberg, L. (1995). Selenium concentrations in brain after exposure to methylmercury: relations between the inorganic mercury fraction and selenium. *Archives of Toxicology*, *69*(4): 228–34.

Branco, V., Canáro, J., Lu, J., Holmgren, A., & Carvalho, C. (2012). Mercury and selenium interaction *in vivo*: Effects on thioredoxin reductase and glutathione peroxidase. *Free Radical Biology & Medicine*, *52*: 781–793.

Brookes, N., & Kristt, D. A. (1989). Inhibition of Amino Acid Transport and Protein Synthesis by HgCl2 and Methylmercury in Astrocytes: Selectivity and Reversibility. *Journal of Neurochemistry*, *53*(4): 1228–1237.

Brown, K. M. & Arthur, J. R. (2001). Selenium, selenoproteins, and human health: a review. *Public Health Nutrition*, *4*(2B): 593–599.

Burk, R. F., Hill, K. E., & Motley, A. K. (2001). Plasma selenium in specific and non-specific forms. *BioFactors*, *14*(1–4): 107–14.

Canty, A. J., Carty, A. J., & Malone, S. F. (1983). Methylmercury(II) Selenolates. Synthesis and Characterization of MeHgSeMe and MeHgSePh, and 1H and 199Hg nmr Studies of Ligand Exchange in MeHg(II) Thiolates and Selenolates, Including Amino Acid Complexes. *Journal of Inorganic Biochemistry*, *19*: 133–142.

Carvalho, C., Chew, E. H., Hashemy, S. I., Lu, J., & Holmgren, A. (2008). Inhibition of the Human Thioredoxin System: A molecular mechanism of mercury toxicity. *The Journal of Biological Chemistry*, *283*(18): 11913–11923.

Carvalho, M., Franco, J., Ghizoni, H., Kobus, K., Nazari, E., Rocha, J., Nogueira, C., Dafre, A., Müller, Y., & Farina, M. (2007). Effects of 2,3-dimercapto-1-propanesulfonic acid (DMPS) on methylmercury-induced locomotor deficits and cerebellar toxicity in mice. *Toxicology*, *239*: 195–203.

Castoldi, A. F., Barni S., Turin I., Gandini C., & Manzo L. (2000). Early acute necrosis, delayed apoptosis and cytoskeletal breakdown in cultured cerebellar granule neurons exposed to methylmercury. *Journal of Neuroscience Research*, *59*: 775–787.

Castoldi, A. F., Johansson, C., Onishchenko, N., Coccini, T., Roda, E., Vahter, M., Ceccatelli, S., & Manzo, L. (2008). Human developmental neurotoxicity of methylmercury: Impact of variables and risk modifiers. *Regulatory Toxicology and Pharmacology*, *51*: 201–214.

Chen, J., & Berry, M. J. (2004). Selenium and selenoproteins in the brain and brain diseases. *Journal of Neurochemistry*, *86*(1): 1–12.

Chen, T., Wong, Y. S., Zheng, W., Bai, Y., & Huang, L. (2008). Selenium nanoparticles fabricated in *Undaria pinnatifida* polysaccharide solutions induce mitochondria-mediated apoptosis in A375 human melanoma cells. *Colloids and Surfaces*, *67*(1): 26–31.

Choi, D. W. (1985). Glutamate neurotoxicity in cortical cell culture is calcium dependent. *Neuroscience letters*, *58*(3), 293–7.

Choi, A. L., Cordier, S., Weihe, P., & Grandjean, P. (2008). Negative confounding in the evaluation of toxicity: the case of methylmercury in fish and seafood. *Critical Reviews in Toxicology*, *38*(10): 877–893.

Clarkson, T. W. & Magos, L. (1966). Studies on the binding of mercury in tissue homogenates. *Biochemical Journal*, *99*: 62–70.

Clarkson T. W., Magos L., & Myers G. J. (2003). The toxicology of mercury – current exposures and clinical manifestations. *The New England Journal of Medicine*, *349*(18): 1731–1737.

Coccini, T., Randine, G., Candura, S. M., Nappi, R. E., Prockop, L. D., & Manzo, L. (2000). Low-level exposure to methylmercury modifies muscarinic cholinergic receptor binding characteristics in rat brain and lymphocytes: physiologic implications and new opportunities in biologic monitoring. *Environmental Health Perspectives*, *108*(1): 29–33.

Cohen, G. & Hochstein, P. (1963). Glutathione peroxidase: the primary agent for the elimination of hydrogen peroxide in erythrocytes. *Biochemistry*, *2*(6): 1420-1427

Compeau, G. C., & Bartha, R. (1985). Sulfate-Reducing Bacteria : Principal Methylators of Mercury in Anoxic Estuarine Sediment, *50*(2).

De Jong, W. H., & Borm, P. J. (2008). Drug delivery and nanoparticles: Applications and hazards. *International Journal of Nanomedicine*, *3*(2): 133–149.

Desai, N. (2012). Challenges in development of nanoparticle-based therapeutics. *The AAPS journal*, *14*(2): 282–95.

Dyrssen, D. & Wedborg, M. (1991). The sulphur-mercury (II) system in natural waters. *Water Air Soil Pollution*, *56*: 507–519.

Evans, L., Garman, R. H., & Weiss, B. (1977). Methylmercury : Exposure duration and regional distribution as determinants of neurotoxicity in nonhuman primates. *Toxicology and Applied Pharmacology*, *41*: 15–33.

Fang, S. C., & Fallin, E. (1976). The binding of various mercurial compounds to serum proteins. *Bulletin of environmental contamination and toxicology*, *15*(1): 110–7.

Farina, M. (2003). Ebselen protects against methylmercury-induced inhibition of glutamate uptake by cortical slices from adult mice. *Toxicology Letters*, *144*(3): 351–357.

Farina, M., Aschner, M., & Rocha, J. B. T. (2011a). Oxidative stress in MeHg-induced neurotoxicity. *Toxicology and applied pharmacology*, *256*(3): 405–17.

Farina, M., Rocha, J. B. T., & Aschner, M. (2011b). Mechanisms of methylmercury-induced neurotoxicity: evidence from experimental studies. *Life sciences*, *89*(15–16): 555–63.

Farina, M., Franco, J., Ribas, C., Meotti, F. C., Missau, F. C., Pizzolatti, M. G., Dafre, A. L., & Santos, A. R. S. (2005). Protective effects of polygala paniculata extract against methylmercury-induced neurtoxicity in mice. *The Journal of Pharmacy and Pharmacology*, 57(11): 1503–1508.

Fitzgerald, W. F., Lamborg, C. H., & Hammerschmidt, C. R. (2007). Marine biogeochemical cycling of mercury. *Chemical Reviews*, *107*(2): 641–62.

Foulkes, E. C. (1993). Metallothionein and glutathione as determinants of cellular retention and extrusion of cadmium and mercury. *Life Sciences*, *52*: 1617–1620.

Franco, J. L., Posser, T., Dunkley, P. R., Dickson, P. W., Mattos, J. J., Martins, R., Bainy, A. C. D., Marques M. R., Dafre A. L., & Farina M. (2009). Methylmercury neurotoxicity is associated with inhibition of the antioxidant enzyme glutathione peroxidase. *Free Radical Biology & Medicine*, *47*(4): 449–57.

Franco, J., Teixeir, A., Meotti, F., Ribas, C. M., Stringari, J., Pomblum, S., Moro A. M., Bohrer D., Bairros A. V., Dafre A. L., Santos A. R. S., & Farina, M. (2006). Cerebellar thiol status and motor deficit after lactational exposure to methylmercury. *Environmental Research*, *102*: 22–28.

Friberg, L. & Mottet, N. (1989) Accumulation of methylmercury and inorganic mercury in the brain. *Biological Trace Element Research*, *21*(1): 201–206.

Friberg, H., Connern, C., Halestrap, A. P., & Wieloch, T. (1999). Differences in the activation of the mitochondrial permeability transition amoung brain regions in the rat correlate with selective vulnerability. *Journal of Neurochemistry, 72*: 2488–2497.

Frisk, P., Yaqob, A., Nilsson, K., Carlsson, J., & Lindh, U. (2000). Uptake and Retention of Selenite and Selenomethionine in cultured K-562 cells. *BioMetals*, *13*: 209–215.

Frisk, P., Yaqob, A., Nilsson, K., & Lindh, U. (2001). Selenite or selenomethionine interaction with methylmercury on uptake and toxicity showing a weak selenite protection: studies on cultured K-562 cells. *Biological trace element research*, *80*(3): 251–68.

Glaser, V., Martins, R. D. P., Vieira, A. J. H., Oliveira, E. D. M., Straliotto, M. R., Mukdsi, J. H., Torres, A. I., de Bem, A. F., Farina, M., da Rocha, J. B. T., De Paul, A. L., & Latini, A. (2014). Diphenyl diselenide administration enhances cortical mitochondrial number and activity by increasing hemeoxygenase type 1 content in a methylmercury-induced neurotoxicity mouse model. *Molecular and Cellular Biochemistry*, *390*(1–2): 1–8.

Götz, M., Koutsilieri, E., Riederer, P., Ceccatelli, S., & Dare, E. (2002). Methylmercury induces neurite degeneration in primary culture of mouse dopaminergic mesencephalic cells. *Journal of Neural Transmission*, *109*: 597–605

Grandjean, P., Weihe, P., White, R. F., Debes, F., Araki, S., Yokoyama, K., Murata, K., Sørensen, N., Dahl, R., Jørgensen, P. J. (1997) Cognitive deficit in 7-year-old children with prenatal exposure to methylmercury. *Neurotoxicology and Teratology*, *19*(6): 417–28.

Hachiya, N. (2012). Chapter 1: Epidemiological Update of Methylmercury and Minamata Disease. *Methylmercury and Neurotoxicity*. Ceccatelli, S. & Aschner, M. (Ed.s), Springer Publications.

Hughes, W. L. (1957). A physiochemical rationale for the biological activity of mercury and its compounds. *Annals of the New York Academy of Sciences*, *65*(5): 454.

Hultberg, B., Andersson, A., and Isaksson, A. (2001). Interaction of metals and thiols in cell damage and glutathione distribution: potentiation of mercury toxicity by dithiothreitol. *Toxicology*, *156*(2–3): 93–100.

Imam, S. Z., Newport, G. D., Islam, F., Slikker, W., & Ali, S. F. (1999). Selenium, an antioxidant, protects against methamphetamine-induced dopaminergic neurotoxicity. *Brain Research*, 575–578.

Jeong, H.Y., Klaue, B., Blum, J.D., & Hayes, K.F. (2007). Sorption of mercuryic ion by synthetic nanocrystalline mackinawite (FeS). *Environmental Science and Technology, 31*(22): 7699–7705.

Johnson, N. C., Manchester, S., Sarin, L., Gao, Y., Kulaots, I., & Hurt, R. H. (2008). Mercury Vapor Release from Broken Compact Fluorescent Lamps and In Situ Capture by New Nanomaterial Sorbents. *Environmental Science & Technology*, *42*(15): 5772–5778.

Juarez, B. I., Martinez, M., Montante, M., Dufour, L., Garcia, E., & Jimenez-Capdeville, M. (2002). Methylmercury increases glutamate extracellular levels in frontal cortex of awake rats. *Neurotoxicology and Teratology*, *24*: 767–771.

Juárez, B. I., Portillo-Salazar, H., González-Amaro, R., Mandeville, P., Aguirre, J. R., & Jiménez, M. E. (2005). Participation of N-methyl-D-aspartate receptors on methylmercury-induced DNA damage in rat frontal cortex. *Toxicology*, *207*(2): 223–9.

Jungblut, M., Tiveron. M.C., Barral, S., Abrahamsen, B., Knobel, F.W., Stoffel, W., Cremer, H., and Bosio, A. (2012) Isolation and characterization of living primary astroglial cell using the new GLAST-specific monoclonal antibody ASCA-1. *GLIA*, *60*: 894–907.

Kajander, E. O., Harvima, R. J., Eloranta, T. O., Martikainen, H., Kantola, M., Kärenlampi, S. O., & Akerman, K. (1991). Metabolism, cellular actions, and cytotoxicity of selenomethionine in cultured cells. *Biological Trace Element Research*, *28*(1): 57–68.

Kaur, P., Aschner, M., Syversen, T. (2006). Glutathione modulation influences methylmercury induced neurotoxicity in primary cell cultures of neurons and astrocytes. *NeuroToxicology*, *27*: 492–500

Kaur, P., Aschner, M., & Syversen, T. (2007). Role of glutathione in determining the differential sensitivity between the cortical and cerebellar regions towards mercury-induced oxidative stress. *Toxicology*, *230*(2–3), 164–77.

Kerper, L., Ballatori, N., & Clarkson, W. (1992). Methylmercury transport across the blood-brain barrier by an amino acid carrier. *American journal of physiology. Regulatory, integrative and Comparative Physiology*, *262*(5): R761–R765.

Khan, M. A. K., Asaduzzaman, A. M., Schrekenbach, G., & Wang, F. (2009). Synthesis, characterization and structures of methylmercury complexes with selenoamino acids. *Dalton Trans*, 5766–5772

Khan, M. A. K. & Wang, F. (2009). Critical Review: Mercury–selenium and their toxicological significance: Toward a molecular understanding of the mercury-selenium antagonism. *Environmental Toxicology and Chemistry*, *28*(8): 1567–1577.

Khan, M. A. K. & Wang, F. (2010). Chemical demethylation of methylmercury by selenoamino acids. *Chemical Research in Toxicology*, *23*(7): 1202–1206

Kidd, K. A., Hesslein, R. H., Fudge, R. J. P., & Hallard, K. A. (1995). The influence of trophic level as measured by &^{15}N on mercury concentrations in freshwater organisms. *Mercury as a Global Pollutant*, 1011–1015.

Kohen, R. & Nyska, A. (2002). Invited Review: Oxidation of Biological Systems: Oxidative stress phenomena, antioxidants, redox reactions, and methods for their quantification. *Toxicologic Pathology*, *30*(6): 620–650.

Komsta-Szumska, E., Reuhi, K., & Miller, D. (1983). Effect of selenium on distribution, demethylation, and excretion of methylmercury by the guinea pig. *Journal of Toxicology and Environmental Health*, *12*(4–6): 775–785.

Korbas, M., O'Donoghue, J., Watson, G., Pickering, I., Singh, S., Myers, G., Clarkson, T., & George, G. (2010). The chemical nature of mercury in human brain following poisoning or environmental exposure. *ACS Chemical Neuroscience*, *1*(12): 810–818.

Limke, T. L., & Atchison, W. D. (2002). Acute Exposure to Methylmercury Opens the Mitochondrial Permeability Transition Pore in Rat Cerebellar Granule Cells. *Toxicology and Applied Pharmacology*, *178*(1): 52–61.

Lin, M.T. & Beal, M.F. (2006). Mitochondrial dysfunction and oxidative stress in neurodegenerative diseases. *Nature*, 443: 787–795.

Lindberg, S. E., Brooks, S., Lin, C. J., Scott, K. J., Landis, M. S., Stevens, R. K., & Richter, A. (2002). Dynamic oxidation of gaseous mercury in the Arctic troposphere at polar sunrise. *Environmental Science & Technology*, *36*(6): 1245–56.

Lockman, P., Mumper, R., Khan, M., & Allen, D. (2002). Nanoparticle Technology for drug delivery across the blood-brain barrier. *Drug Development and Industrial Pharmacy*, *28*(1): 1–13.

Lopez-Heras, I., Sanchez-Diaz, R., Anunciacao, D. S., Madrid, Y., Luque-Garcia, J., & Camara, C. (2014). Effect of Chitosan-stabilized Selenium nanoparticles on cell cycle arrest and invasiveness in hepatocarcinoma cells revealed by quantitative proteomics. *Nanomedicine & Nanotechnology*, *5*(5).

Machado, M. C., Cheng, D., Tarquinio, K. M., & Webster, T. J. (2010). Nanotechnology: pediatric applications. *Pediatric Research*, *67*(5): 500–4.

Mailloux, R. J., Xuan, J. Y., McBride, S., Maharsy, W., Thorn, S., Holterman, C. E., Kennedy, C. R. J., Rippstein, P., deKemp, R., da Silva, J., Nemer, M., Lou, M., & Harper, M. E. (2014) Glutaredoxin-2 is required to control oxidative phosphorylation in cardiac muscle by mediating deglutathionylation reactions. *Journal of Biological Chemistry, 289*: 14812–14828.

Manke, A., Wang, L., & Rojanasakul, Y. (2013) Mechanisms of Nanoaprticle-induced oxidative stress and toxicity. *BioMed Research International*

Marek, R., Caruso, M., Rostami, A., Grinspan, J. B., & Sarma, J. D. (2008). Magnetic cell sorting: a fast and effective method of concurrent isolation of high purity viable astrocytes and microglia from neonatal mouse brain tissue. *Journal of Neuroscience Methods*, *175*(1): 108–18.

Migliore, L. & Coppedè, F. (2009). Environmental-induced oxidative stress in neurodegenerative disorders and aging. *Mutation Research*, *674*: 73–84.

Mitka, M. (2008). Chelation Therapy Trials Halted. *Journal of the American Medical Association*, *300*(19): 2236.

Morken, T. S., Sonnewald, U., Aschner, M., & Syversen, T. (2005). Effects of methylmercury on primary brain cells in mono- and co-culture. *Toxicological Sciences*, *87*(1): 169–75.

Mori, N., Yasutake, A., & Hirayama, K. (2007). Comparative study of activities in reactive oxygen species production/defense system in mitochondria of rat brain and liver, and their susceptibility to methylmercury toxicity. *Archives of Toxicology, 81*: 769–776.

Mutkus, L., Aschner, J. L., Syversen, T., & Aschner, M. (2005). Methylmercury alters the in vitro uptake of glutamate in GLAST- and GLT-1-transfected mutant CHO-K1 cells. *Biological Trace Element Research*, *107*(3): 231–45.

Ni, M., Li, X., Yin, Z., Sidoryk-Wegrzynowicz, M., Jiang, H., Farina, M., Rocha, J. B., Syversen, T., & Aschner, M (2011). Comparative study on the response of rat primary astrocytes and microglia to methylmercury toxicity. *GLIA*, *59*: 810–820.

Nishikido, N., Furuyashiki, K., Naganuma, A., Suzuki, T., & Imura, N. (1987). Maternal selenium deficiency enhances the fetolethal toxicity of methyl mercury. *Toxicology and Applied Pharmacology*, *88*(3): 322–8.

Nordberg, J., & Arnér, E. S. J. (2001). Reactive oxygen species, antioxidants, and the mammalian thioredoxin system, *Free Radical and Biological Medicine, 31*: 1287–1312.

Ohi, G., Nishigaki, S., Seki, H., Tamura, Y., Maki, T., Maeda, H., Ochiai, S., Yamada, H., Shimamura, Y., & Yagyu, H. (1975). Interaction of dietary methylmercury and selenium on accumulation and retention of these substances in rat organs. *Toxicology and Applied Pharmacology*, *32*: 527–533.

Paglia, D. E. & Valentine, W. N. (1967). Studies on the quantitative and qualitative characterization of erythrocyte glutathione peroxidase. *Journal of Laboratory and Clinical Medicine 70*(1): 158–169.

Palmisano, F., Cardellicchio, N., & Zambonin, P. G. (1995). Speciation of mercury in dolphin liver: a two-stage mechanism for the demethylation accumulation process and role of selenium. *Marine Environmental Research*, *40*(2): 109–121.

Petersen, M. S., Weihe, P., Choi, A., & Grandjean, P. (2008a). Increased prenatal exposure to methylmercury does not affect the risk of Parkinson's disease. *Neurotoxicology*, *29*(4): 591–5.

Petersen, M. S., Halling, J., Bech, S., Wermuth, L., Weihe, P., Nielsen, F., Jorgensen, P. J., Budtz-Jorgensen, B., & Grandjean, P. (2008b). Impact of dietary exposure to food contaminants on the risk of Parkinson's disease. *Neurotoxicology*, *29*(4), 584–90.

Rabenstein, D. L., & Reid, R. S. (1984). Nuclear Magnetic Resonance Studies of the Solution Chemistry of Metal Complexes. 20. Ligand-Exchange Kinetics of Methylmercury(II)-Thiol Complexes. *Inorganic Chemistry*, *23*(6): 1246–1250.

Ralston, N. V. C., Azenkeng, A., & Raymond, L. J. (2012). Mercury-dependent inhibition of selenoenzymes and mercury toxicity. In S. Ceccatelli & M. Aschner (ed.s), *Chapter 5: Methylmercury and Neurotoxicity* (pp. 91–99).

Roos, D., Puntel, R., Santos, M., Souza, D., Farina, M., Nogueira, C., Aschner, M., Burger, M., Barbosa, N., Rocha, J. (2009). Guanosine and synthestic organoselenium compounds modulate methylmercury-induced oxidative stress in rat brain cortical slices: Involvement of oxidative stress and glutamatergic system. *Toxicology In Vitro*, *23*: 302–307.

Sanchez, V., Camarero, J., O'Shea, E., Green, A., & Colado, M. (2003). Differential effect of dietary selenium on the long-term neurotoxicity induced by MDMA in mice and rats. *Neuropharmacology*, *44*(4): 449–461.

Sanfeliu, C., Sebastia, J., & Kim, S. (2001). Methylmercury neurotoxicity in cultures of human neurons, astrocytes, neuroblastoma cells. *NeuroToxicology*, *22*: 317–327

Savaskan, N. E., Bräuer, A. U., Kühbacher, M., Eyüpoglu, I. Y., Kyriakopoulos, A., Ninnemann, O., Behne D., & Nitsch, R. (2003). Selenium deficiency increases susceptibility to glutamate-induced excitotoxicity. *FASEB Journal*, *17*(1): 112–4.

Schweizer, U, Bräuer, AU, Köhrle, J, Nitsch, R, & Savaskan, NE (2004). Selenium and brain function: a poorly recognized liaison. *Brain research. Brain Research Reviews*, *45*(3): 164–78.

Scott, B. R. (2012). Are some neurons hypersensitive to metallic nanoparticles? *Dose-Response*, *10*: 37–57.

Selin, N. E. (2009). Global biogeochemical cycling of mercury: A Review. *Annual Review of Environment and Resources*, *34*: 43–63.

Shakibaie, M., Shahverdi, A. R., Faramarzi, M. A., Hassanzadeh, G. R., Rahimi, H. R., & Sabzevari, O. (2013). Acute and subacute toxicity of novel biogenic selenium nanoparticles in mice. *Pharmaceutical Biology*, *51*(1): 58–63.

Shanker, G., & Aschner, M. (2001). Identification and characterization of uptake systems for cystine and cysteine in cultured astrocytes and neurons: evidence for methylmercury-targeted disruption of astrocyte transport. *Journal of Neuroscience Research*, *66*(5): 998–1002.

Shanker, G., Aschner, J. L., Syversen, T., & Aschner, M. (2004). Free radical formation in cerebral cortical astrocytes in culture induced by methylmercury. *Brain Research*, *128*(1): 48–57.

Shapiro A. M. & Chan H. M. (2008). Characterization of demethylation of methylmercury in cultured astrocytes. *Chemosphere*, *74*(1): 112–118.

Simmons-Willis, T. A., Koh, A. S., Clarkson, T. W., Ballatori, N. (2002).Transport of a neurotoxicant by molecular mimicry: The methylmercury-L-cysteine complex is a substrate for human L-type large neutral amino acid transporter (LAT) 1 and LAT2. *Biochem Journal, 367*: 239–246.

Simpson, R. B. (1961). Association constants of methylmercury with sulfhydryl and other bases. *Journal of the American Chemical Society*, *83*(23): 4711.

Skyllberg, U. & Drott, A. (2010). Competition between disordered iron sulfide and natural organic matter associated thiols for mercury (II) – an EXAFS study. *Environmental Science and Technology, 44*: 1254–1259.

Smith, I. K., Vierheller, T. L., & Thorne, C. A. (1988). Assay of glutathione reductase in crude tissue homogenate using 5,5`dithiobis(2-nitrobenzoic acid). *Analytical Biochemistry, 175*: 408–413.

Sokolowski, K., Falluel-Morel, A., Zhou, X., & DiCicco-Bloom, E. (2011). Methylmercury (MeHg) elicits mitochondrial-dependent apoptosis in developing hippocampus and acts at low exposures. *Neurotoxicology*, *32*(5): 535–44.

Sorensen, N., Murata, K., Budtz-Jorgensen, E., Weihe, P., & Grandjean, P. (1999). Prenatal methyl-mercury exposure as a cardiovascular risk factor at seven years of age. *Epidemiology*, *10*: 370–5.

Steinbrenner, H., Alili, L., Bilgic, E., Sies, H., & Brenneisen, P. (2006). Involvement of selenoprotein P in protection of human astrocytes from oxidative damage. *Free radical Biology & Medicine*, *40*(9): 1513–23.

Steinmann, D., Nauser, T., & Koppenol, W. K. (2010). Selenium and sulfur in exchange reactions: a comparative study. *Journal of Organic Chemistry*, *75*(19): 6696–6699.

Steuerwald, U., Weibe, P., Jørgensen, P. J., Bjerve, K., Brock, J., Heinzow, B., Budtz-Jørgensen, E., & Grandjean P. (2000). Maternal seafood diet, methylmercury exposure, and neonatal neurologic function. *The Journal of Pediatrics*, *136*(5): 599–605.

Sumathi, T., Shobana, C., Christinal, J., & Anusha, C. (2012). Protective effect of Bacopa monniera on methyl mercury-induced oxidative stress in cerebellum of rats. *Cellular and Molecular Neurobiology*, *32*(6): 979–87.

Trapp, G., & Millam, J. (1975). Distribution of 75-Se in brains of selenium-deficient rats. *Journal of neurochemistry*, *24*: 593–595.

UNEP (2013a). Global Mercury Assessment 2013: Sources, Emissions, Releases and Environmental Transport. UNEP Chemial Branch, Geneva, Switzerland.

UNEP (2013b). Report of the intergovernmental negotiating committee to prepare a global legally binding intrument on mercury on the work of its fifth sessions. Retrieved 07/11/1013 from <http://www.unep.org/hazardoussubstances/Mercury/Negotiations/INC5/INC5Report/tabid/3496/Default.aspx>

US EPA (2001). Methylmercury (MeHg) (SASRN 22967-92-6). *Integrated Risk Information System*. Found Online 16/10/2012 from <http://www.epa.gov/iris/subst/0073.htm>

US FDA (2013). Mercury Levels in Commercial Fish and Shellfish (1990–2010). *US Department of Health & Human Services*. Found Online 22/11/13 from <http://www.fda.gov/food/foodborneillnesscontaminants/metals/ucm115644.htm>

Verma, A. & Stellacci, F. (2010). Effect of surface properties on nanoparticle-cell interactions. *Small*, 6(1): 12–21.

Vizuete, M. L., Steffen, V., Machado, A., & Cano, J. (1994). 1-Methyl-4-phenylpyridinium has greater neurotoxic effect after selenium deficiency than after vitamin E deficiency in rat striatum. *European Journal of Pharmacology*, *270*: 183–187.

Wakabayashi, K., Kakita, A., Sakamoto, M., Su, M., Iwanaga, K., & Ikuta, F. (1995). Variability of brain lesions in rats administered methylmercury at various postnatal development phases. *Brain Research*, *705*(1–2): 267–72.

Watanabe, C., Yin, K., Kasanuma, Y., & Satoh, H. (1999). In utero exposure to methylmercury and Se deficiency converge on the neurobehavioral outcome in mice. *Neurotoxicology and Teratology*, *21*(1): 83–8.

Witte, M., Geurts, J., de Vries H., van der Valk, P., & von Horssen, J. (2010). Mitochondrial dysfunction: A potential link between neuroinflammation and neurodegeneration? *Mitochondrion*, *10*: 411–418.

Wu, H., Li, X., Liu, W., Chen, T., Li, Y., Zheng, W., Man, C. W. Y., Wong, M. K., & Wong, K. H. (2012). Surface decoration of selenium nanoparticles by mushroom polysaccharides–protein complexes to achieve enhanced cellular uptake and antiproliferative activity. *Journal of Materials Chemistry*, *22*(19): 9602.

Xia T., Kovochich M., Brant J., Hotze M., Sempf J., Oberley T., Sioustas C., Yeh J. I., Wiesner M. R., & Nei A. E. (2006). Comparison of the abilities of ambient and manufactured nanoparticles to induce cellular toxicity according to an oxidative stress paradigm. *Nano Letters*, *6*(8): 1794–1807.

Xia, T., Li, N., & Nel, A.E. (2009). Potential Health impact of nanoparticles. *Annual Review of Public Health*, *30*: 137–150.

Xu F.F. & Implay J.A. (2012). Silver (I), Mercury (II), Cadmium (II), and Zinc (II) target iron-sulfur clusters when they toxify *Escherichia coli*. *Applied Environmental Microbiology*, *78*(10): 3614–3621.

Xu, B., Xu, Z. F., Deng, Y., Liu, W., Yang, H. B., & Wei, Y. G. (2012). Protective effects of MK-801 on methylmercury-induced neuronal injury in rat cerebral cortex: involvement of oxidative stress and glutamate metabolism dysfunction. *Toxicology*, *300*(3), 112–20.

Yamamoto, R., Suzuki, T., Satoh, H., & Kawai, K. (1986). Generation and dose as modifying factors of inorganic mercury accumulation in brain, liver, and kidneys of rats fed methylmercury. *Environmental Research, 41*: 309–318.

Yamashita, M., Yamashita, Y., Suzuki, T., Kani, Y., Mizusawa, N., Imamura, S., & Touhata, K. (2013). Selenoneine, a novel selenium-containing compound, mediates detoxification mechanisms against methylmercury accumulation and toxicity in zebrafish embryo. *Marine Biotechnology*, *15*(5): 559–70.

Yang F, Tang, Q, Zhong, X, Bai, Y, Chen, T, Zhang, Y, Li, Y, Zheng, W (2012). Surface decoration by Spirulina polysaccharide enhances the cellular uptake and anticancer efficacy of selenium nanoparticles. *International Journal of Nanomedicine*, 7: 835–844.

Yin, Z., Milatovic, D., Aschner, J. L., Syversen, T., Rocha, J. B. T., Souza, D. O., Sidoryk, M., Albrecht J., & Aschner, M. (2007). Methylmercury induces oxidative injury, alterations in permeability and glutamine transport in cultured astrocytes. *Brain Research*, *1131*(1): 1–10.

Zemolin, A., Meinerz, D., de Paula, M., Mariano, D., Rocha, J., Pereira, A., Posser T., & Franco, J. (2012). Evidences for a role of glutathione peroxidase 4 (GPx4) in methylmercury induced neurotoxicity in vivo. *Toxicology*, *302*(1): 60–7.

Zhang, S., Rocourt, C., & Cheng, W. H. (2010). Selenoproteins and the aging brain. *Mechanisms of Ageing and Development*, *131*(4): 253–260.

Zhang, Y., Li, X., Huang, Z., Zheng, W., Fan, C., & Chen, T. (2013). Enhancement of cell permeabilization apoptosis-inducing activity of selenium nanoparticles by ATP surface decoration. *Nanomedicine*, *9*(1): 74–84.

Zhang L., Zhang M., Dong J., Guo J., Song Y., and Cheung K. (2001). Chemical structure and chain conformation of the water-insoluble glucan isolated from Pleurotus tuber-regium. *Biopolymers*, *59*: 457–464.

Appendices

Appendix A: Animal ethics training

Proof of completion of the CCAC and NIAUT animal ethics training at University of Ottawa required before beginning animal research based on the approved protocol BL-270 (signatures removed to maintain confidentiality).